

1 **Fine-scale source apportionment of PM₁₀ with new organic tracers in**
2 **three urban sites in a metropolitan area in France**

3 Lucille Joanna S. Borlaza¹, Samuël Weber¹, Gaëlle Uzu^{1*}, Véronique Jacob¹, Trishalee Cañete¹, Olivier
4 Favez², Steve Micallef³, Cécile Trébuchon³, Rémy Slama⁴, and Jean-Luc Jaffrezo¹

5 ¹University Grenoble Alpes, CNRS, IRD, INP-G, IGE (UMR 5001), 38000 Grenoble, France

6 ²INERIS, Parc Technologique Alata, BP 2, 60550 Verneuil-en-Halatte, France

7 ³AtmoAuvergne-Rhônes Alpes, 38400 Grenoble, France

8 ⁴IAB, Team of Environmental Epidemiology applied to Reproduction and Respiratory Health, University of Grenoble Alpes,
9 38000 Grenoble, France

10 *Correspondence to: Gaëlle Uzu (gaelle.uzu@ird.fr)

11 **Abstract.** A fine-scale source apportionment of PM₁₀ was conducted in three different urban sites (background, hyper-
12 center, and peri-urban) within 15 km of the city in Grenoble, France using Positive Matrix Factorization (PMF 5.0) on
13 measured chemical species from collected filters (24-hr) from February 2017 to March 2018. Several new organic tracers (3-
14 MBTCA, pinic acid, phthalic acid, MSA, and cellulose) were additionally used in order to identify sources that are
15 commonly unresolved. An 11-factor solution was obtained in all sites including commonly identified sources from primary
16 traffic, nitrate-rich, sulfate-rich, industrial, biomass burning, aged sea salt, sea/road salt, and mineral dust, and the newly
17 found sources from primary biogenic, secondary biogenic oxidation, and MSA-rich. Generally, the chemical species
18 exhibiting similar temporal trends and strong correlations showed uniformly distributed emission sources in the Grenoble
19 basin. The PMF model was able to obtain and differentiate chemical profiles of specific sources even at high proximity of
20 receptor locations confirming its applicability in a fine-scale resolution. In order to test the similarities between the PMF-
21 resolved sources, the Pearson distance and standardized identity distance (PD-SID) of the factors in each site were
22 compared. The PD-SID metric determined homogeneous sources (biomass burning, primary traffic, nitrate-rich, sulfate-rich,
23 primary biogenic, MSA-rich, aged sea salt, and secondary biogenic oxidation) and heterogeneous sources (industrial, mineral
24 dust, and sea/road salt) across different urban sites, thereby allowing to better discriminate localized characteristics of
25 specific sources. Overall, the addition of the new tracers allowed the identification of substantial sources (especially in the
26 SOA fraction) that would not have been identified or possibly mixed with other factors, resulting in an enhanced resolution
27 and sound source profile of urban air quality at a city scale.

29 **1 Introduction**

30 Atmospheric aerosols, or particulate matter (PM), are complex mixtures of particles from direct and indirect emissions (e.g.,
31 gas-to-particle conversion processes) that are from natural and anthropogenic sources in the atmosphere (Wilson and
32 Spengler, 1996). The growing interest in ambient aerosol studies is driven by their impacts on health, air quality, and global
33 climate (Colette et al., 2008; Horne and Dabdub, 2017; McNeill, 2017; Shiraiwa et al., 2017). Numerous epidemiological
34 studies have established consistent associations between PM and various health diseases, especially cardiorespiratory
35 illnesses (Brunekreef, 2005; Franchini and Mannucci, 2009; Langrish et al., 2012; Ostro et al., 2011; Willers et al., 2013).
36 Hence, current efforts are focused on determining emission sources in order to properly instigate the reduction of ambient
37 PM mass concentrations to regulation limits. However, determining the contribution of emission sources is often a
38 challenging task.

39 The applicability of receptor models to extract information by variable reduction techniques, especially in large datasets,
40 demonstrated its ability in different branches of scientific research. The Positive Matrix Factorization (PMF) model is one
41 approach used in many studies to determine the contribution of emission sources in PM, based on the characterization of
42 chemical tracers in a series of PM samples (Belis et al., 2014, 2020; Hopke, 2016; Pindado and Perez, 2011; Saeaw and
43 Thepanondh, 2015; Weber et al., 2019). The option of refining source profiles by adding constraints have further improved
44 the accuracy of identifying sources (Marmur et al., 2007; Weber et al., 2019; Zhu et al., 2018), especially when specific
45 chemical species and unique tracers are included (Bullock et al., 2008).

46 The wide and complex range of chemical components in PM is largely due to the organic fraction (Seinfeld and Pankow,
47 2003) which typically ranges from 10% to 90% of its total mass, consisting of complex mixtures especially in urban
48 environments (Schauer and Cass, 2000; Zheng et al., 2004). In fact, around 80% of organic matter (OM) generally remains
49 unidentified at the molecular level (Chevrier, 2016; Golly et al., 2019) resulting in misclassification or several un-
50 apportioned sources of PM₁₀. Additionally, the difference in formation pathways of PM components may limit the
51 identification of sources of PM, especially the secondary organic carbon (SOC) fraction, without the use of relevant organic
52 tracers (Wang et al., 2017a). While some organic tracers have already been integrated in previous studies using PMF model
53 (Belis et al., 2019; Golly et al., 2019; Hu et al., 2010; Srivastava et al., 2018b; Weber et al., 2019), some key tracers have not
54 been explored yet, especially for commonly unresolved sources, such as biogenic aerosols and products of secondary
55 processes in the atmosphere, even if some recent studies took anthropogenic secondary organic aerosols (SOA) into account
56 (Srivastava et al., 2018b). Furthermore, the usefulness of these organic tracers requires further methodological exploration of
57 the PMF capabilities, both in terms of proper source tracers, and also in relation to the small scale variability of their
58 concentrations. Indeed, although the PMF model showed good strengths in both rural and urban environments (Pindado and
59 Perez, 2011; Schauer and Cass, 2000), it has never been used in cities at a fine-scale resolution allowing to test its ability to
60 assess the local variabilities in an urban area. This is, however, a research area in expansion (Dai et al., 2020b, 2020a;
61 Pandolfi et al., 2020).

62 The city of Grenoble (France), with a complex topography and marked seasonal cycles of particulate pollution, offers
63 interesting opportunities to explore the capability of PMF to resolve both the small spatial and large temporal scales of
64 variabilities of the contribution of PM sources with the possibility of using additional tracers. Specific meteorological
65 conditions, topography, and local sources impact the local PM chemistry in the atmosphere thereby requiring additional
66 sources to properly scrutinize these local variations in urban environments. Further, previous works were already conducted
67 in the area using extended PMF (Srivastava et al., 2018b; Weber et al., 2018), providing good benchmarks.

68 In this paper, we present results of a study conducted over one year at three sites within 15 km of each other, in the Grenoble
69 metropolitan area. The sources of PM_{10} were apportioned using measured common chemical components including organic
70 and elemental carbon, ions, specific tracers in the carbonaceous matter (anhydride monosaccharides, polyols, MSA), and
71 metals. Additionally, organic species including free cellulose, and several organic acids were also measured to improve the
72 input dataset in the PMF model and to tackle known sources not commonly identified in PMF studies. Further, this work also
73 focuses on the spatial and seasonal variabilities in the source contributions for different urban typologies inside the
74 metropolitan area, in order to test the capability of the PMF approach to handle this diversity of situations. This could be a
75 key tool to policy makers in providing vital information for designing effective particulate matter control strategies at a city
76 scale, including the setup of low emission zones.

77 **2 Methodology**

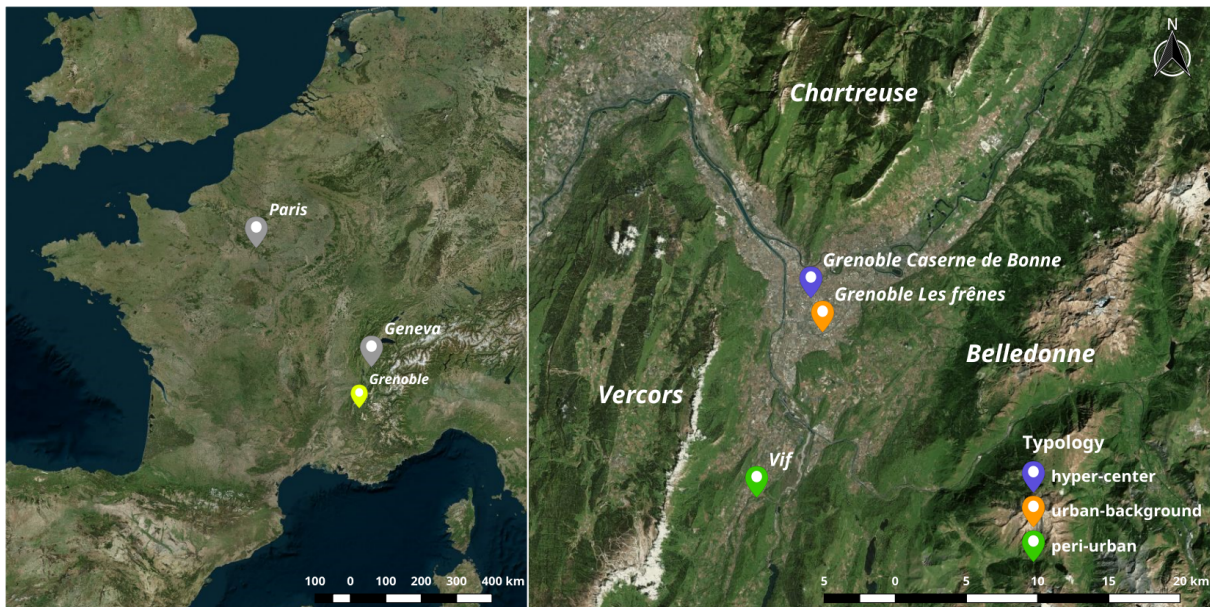
78 **2.1 PM_{10} sample collection**

79 The city of Grenoble, regarded as the capital of the French Alps, is located in an alpine environment (Figure 1) but the city
80 itself presents a low altitude range between 204-600 masl and its metropolitan area has a population of about 440,000
81 inhabitants. Several mountain ranges surround the city including Chartreuse (north), Vercors (south and west), and
82 Belledonne (east), thereby heavily affecting the local meteorology. The surrounding mountains restrict the movement of air
83 resulting to the development of atmospheric temperature inversions, hence an entrapment of pollutants in the valley
84 particularly in winter. During this study, a sampling campaign for PM_{10} was conducted in the Grenoble area at three sites
85 selected to represent various urban typologies, including: Les Frênes (LF, urban background site), Caserne de Bonne (CB,
86 urban hyper-center), and Vif (peri-urban area). These sites are all within a 15-km range from the city center. LF is an urban
87 background reference site for the Air Quality agency, nearby a park at the outer fringe of the city. Vif is a peri-urban site,
88 with suburban housings close to rural areas. However, this site could potentially receive industrial emissions because of a
89 nearby chemical industrial area (<6 km) in the air flux within this North – South valley. Biogenic emissions also could be
90 expected as this site is in-between the foot of Vercors and Belledone national parks. Lastly, while in a pedestrian area, the
91 site of CB is in the hyper-center of Grenoble and exposed to traffic emissions from the nearby boulevards.

92 The daily (24-h) PM_{10} sampling collection was conducted from February 28, 2017 to March 10, 2018 (starting at 00:00 local
93 time) with an average 3-day sampling interval. A total of 125, 127 and 127 samples were collected during this year-long

94 campaign at the Air Quality Network stations of LF, CB, and Vif, respectively. The PM₁₀ collection was performed using
95 high volume samplers (Digitel DA80, 30 m³ h⁻¹) onto 150 mm-diameter quartz fibre filters (Tissu-quartz PALL QAT-UP
96 2500 diameter 150 mm). Filters were preheated at 500 °C for 12 hours before use to avoid organic contamination. At least 20
97 blank filters were collected from each site to determine detection limits (DL) and to secure the absence of contamination
98 during sample transport, setup, and recovery. Within one week of collection, all filter samples were wrapped in aluminium
99 foil, sealed in zipper plastic bags, and stored at <4 °C until further chemical analysis. All handling procedures of filters were
100 strictly under quality control to avoid any possible contamination. Additional information came from the same stations,
101 including the PM₁₀ mass measured with a tapered element oscillating microbalance and filter dynamics measurement system
102 (TEOM-FDMS).

103



104
105 **Figure 1: Grenoble, the city where the sampling was made, placed on a European Map (left), and PM monitoring sites (right): Les
106 Frênes or LF (background), Caserne de Bonne or CB (hyper-center), and Vif (peri-urban). Image credit: Bing™ Aerial.**

107

108 2.2 Classical set of chemical analyses

109 After collection, samples were subjected to various chemical analyses in order to perform the quantification of the major
110 constituents by mass and specific chemical tracers of sources needed for PMF studies.
111 The carbonaceous components (organic carbon (OC) and elemental carbon (EC)) were analysed using a thermo-optical
112 method on a Sunset Lab analyser (Aymoz et al., 2007; Birch and Cary, 1996), using the EUSAAR2 temperature program
113 (Cavalli et al., 2010). Total organic matter (OM) in daily ambient aerosols were estimated by multiplying the OC mass by a

fixed factor, OM=1.8×OC (Favez et al., 2010; Putaud et al., 2010). This factor is in agreement with a determination performed during the FORMES program in the Grenoble area with AMS measurements (Favez et al., 2010). All aqueous analyses were conducted on the same fraction of the filter, using one 11.34 cm² punch per sample. A solid/liquid extraction was performed in a 10 ml of ultra-pure water under vortex agitation for 20 minutes. The extract was then filtered with a 0.25 µm porosity Acrodisc (Milipore Millex-EIMF) filter. The major ionic components are measured by ion chromatography (IC) following a standard protocol described in Jaffrezo et al. (1998) and Waked et al. (2014), using an ICS3000 dual channel chromatograph (Thermo-Fisher) with AS11HC column for the anions and CS12 for the cations. This technique allowed the quantification of the ions sodium (Na⁺), ammonium (NH₄⁺), potassium (K⁺), magnesium (Mg²⁺), calcium (Ca²⁺), chloride (Cl⁻), nitrate (NO₃⁻), sulfate (SO₄²⁻), and methane sulfonic acid (MSA). The analyses of anhydro-sugars and primary saccharides were achieved using a High Performance Liquid Chromatography with Pulsed Amperometric Detection (HPLC-PAD). This is performed with a Thermo-Fisher ICS 5000⁺ HPLC equipped with 4 mm diameter Metrosep Carb 2×150 mm column and 50 mm pre-column. The analytical run is isocratic with 15% of an eluent of sodium hydroxide (200 mM) and sodium acetate (4 mM) and 85% water, at 1 ml min⁻¹. This method allowed the quantification of anhydrous saccharides (levoglucosan and mannosan), polyols (arabitol and mannitol), and glucose (Samake et al., 2018; Waked et al., 2014). Trace elements were analysed after mineralization of a 38 mm diameter punch of each filter, using 5 ml of HNO₃ (70%) and 1.25 ml of H₂O₂ during 30 minutes at 180 °C in a microwave oven (microwave MARS 6, CEM). The analysis of 18 trace elements (Al, As, Ba, Cd, Cr, Cu, Fe, Mn, Mo, Ni, Pb, Rb, Sb, Se, Sn, Ti, V, and Zn) was performed on this extract using inductively coupled plasma mass spectroscopy (ICP-MS) (ELAN 6100 DRC II PerkinElmer or NEXION PerkinElmer) in a way similar to that described by Alleman et al. (2010).

2.3 Additional set of analysis of organic tracers

2.3.1 Organic acids analysis

The analysis of a large array of organic acids (including pinic and phthalic acids, and 3-MBTCA) was conducted on the same water extracts used for IC and HPLC-PAD analyses. In brief, it was performed with an HPLC-MS system (GP40 Dionex with a LCQ-FLEET Thermos-Fisher ion trap), with the electrospray ionization in the negative mode. The separation column is a Synergi 4 µm Fusion – RP 80A (250×3 mm ID, 4 µm particle size, from Phenomenex). An elution gradient was optimized for the separation of the compounds, with a binary solvent gradient consisting of 0.1% formic acid in acetonitrile (solvent A) and 0.1% aqueous formic acid (solvent B) in various proportions during the 40-minute analytical run. Column temperature was maintained to 30 °C. Eluent flow rate was 0.5 ml min⁻¹, and injection volume was 250 µl. Calibrations were performed for each analytical batch with solutions of authentic standards. All standards and samples were spiked with internal standards (phthalic-3,4,5,6-d⁴ acid and succinic-2,2,3,3-d⁴ acid). The calculation of the final atmospheric

145 concentrations was corrected with the concentrations of internal standards and of the procedural blanks, taking also into
146 account the extraction efficiency varying between 76-116% according to the acid.

147 **2.3.2 Cellulose analysis**

148 The concentration of atmospheric cellulose was quantified using improvements of the procedure proposed by Kunit and
149 Puxbaum (1996). The principle is to extract the cellulose from the filter in an aqueous solution, then to process this extract in
150 several solutions of enzymes in order to break-down the cellulose into glucose units, and finally to quantify the glucose
151 concentrations using an HPLC-PAD technique. In brief, a 21 mm diameter punch of each quartz filter sample is extracted for
152 40 minutes using an ultrasound bath in 3 ml of an aqueous solution with thymol buffer (pH 4.8). Then two enzymes
153 solutions (cellulase (Sigma Aldrich, C2730) with 20 µl of an aqueous solution at 70 units g⁻¹) and glucosidase (Sigma
154 Aldrich, 49291), with 60 µl of an aqueous solution at 5 units g⁻¹) are added into the solution. The solution is then incubated at
155 50 °C for 24 hours for the hydrolysis to occur. The hydrolysis is stopped by placing the solution in an oven at 100 °C for 45
156 minutes. The solution is then centrifuged (7000 rpm) for 15 minutes, and carefully extracted out using a syringe before being
157 analysed with an HPLC-PAD instrument. The procedural blanks are greatly improved when the enzymes stock solution are
158 filtered to lower their glucose content. This is performed with a series of cleaning steps (n=10) by tangential ultrafiltration in
159 a Vivaspin 15R tube at 7000 rpm in Milli-Q water.

160 The HPLC-PAD (Dionex DX500) is equipped with a Methrom column (250 mm long, 4 mm diameter), with an isocratic run
161 of 40 minutes with the eluents A (50%, 18mM NaOH), B (25%, 100 mM NaOH + 150mM NaAc), and C (25%, 220 mM
162 NaOH). Column temperature is maintained at 30 °C. Eluent flow rate is 1 ml min⁻¹, and injection volume is 250 µl. Each
163 analytical batch also includes standard glucose solutions as well as standard cellulose solutions (using 20 µm beads, Sigma
164 Aldrich, S3504) that have been processed like the real samples in order to determine the specific efficiency of the cellulose-
165 to-glucose enzymatic conversion for each batch. The final calculation of the atmospheric concentration of the free cellulose
166 takes this conversion efficiency into account. It varied according to the batch, generally ranging from 65–80%. The
167 calculation of the cellulose concentration also takes into account the initial concentrations of atmospheric glucose of each
168 sample, determined in parallel with the HPLC-PAD analysis of sugars and polyols as described above. Finally, field and
169 procedural blanks are also taken into account.

170 **2.4 Source apportionment**

171 **2.4.1 Input species of PMF**

172 Source apportionment of PM₁₀ was conducted using the United States Environmental Protection Agency (US-EPA) software
173 PMF 5.0 (Norris et al., 2014), aiming at the identification and quantification of the major sources of PM₁₀ for the three urban
174 sites in the Grenoble basin. PMF is based on the factor analysis technique (Paatero and Tapper, 1994). Briefly, PMF is based
175 on a weighted least-squares fit algorithm allowing the resolution of Eq. S1 (cf the supplementary information (SI)). In our

176 study, 35 chemical species were used as input variables, namely OC*, EC, ions (Na^+ , K^+ , NH_4^+ , Mg^{2+} , Ca^{2+} , NO_3^- , SO_4^{2-} and
 177 Cl^-), trace metals (Al, As, Cd, Cr, Cu, Fe, Mn, Mo, Ni, Pb, Rb, Sb, Se, Sn, Ti, V and Zn) and organic markers (MSA,
 178 levoglucosan, mannosan, polyols (sum of arabitol and mannitol), pinic acid, 3-MBTCA, phthalic acid, and cellulose), as
 179 summarized in Table S1 in SI. We assumed that arabitol and mannitol originated from the same source, and hence combined
 180 them into one component labelled as “polyols” (Samaké et al., 2019). In order to avoid double counting of carbon mass, OC*
 181 was calculated using Eq. S2. The uncertainties of the input variables were calculated using Eq. S3 (Gianini et al., 2012).
 182 Finally, the species displaying a signal-to-noise ratio (S/N) lower than 0.2 were discarded and those with S/N between 0.2
 183 and 2 were classified as “weak” (3-fold uncertainties).

184 **2.4.2 Set of constraints**

185 Since mixing issues between factors are inherent to PMF (i.e., collinearity due to meteorological conditions) and to possible
 186 rotational ambiguity in the solution, we applied a set of constraints to the selected best base case solutions thanks to the ME-
 187 2 solver (Paatero, 1999). On top of the constraints defined in Weber et al. (2019), who applied a minimum set of constraints
 188 to a large series of data sets within the SOURCE program, we added specific constraints for the traffic factor, derived from a
 189 previous study in Grenoble dedicated to traffic emissions (Charron et al., 2019), as summarized in Table 1. These constraints
 190 were applied similarly to the data sets from the 3 sites. This allows the orientation of the PMF solution towards more stable
 191 and environmentally realistic profiles.
 192

193 **Table 1: Summary of the applied chemical constraints on source-specific tracers in the PMF factor profiles.**

Factor profile	Element	Type	Value
Biomass burning	Levoglucosan	Pull up maximally	(% dQ 0.50)
Biomass burning	Mannosan	Pull up maximally	(% dQ 0.50)
Primary biogenic	Levoglucosan	Set to zero	0
Primary biogenic	Mannosan	Set to zero	0
Primary biogenic	Polyols	Pull up maximally	(% dQ 0.50)
Primary biogenic	EC	Pull down maximally	(% dQ 0.50)
MSA-rich	MSA	Pull up maximally	(% dQ 0.50)
MSA-rich	Levoglucosan	Set to zero	0
MSA-rich	Mannosan	Set to zero	0
MSA-rich	Polyols	Pull down maximally	(% dQ 0.50)
MSA-rich	EC	Pull down maximally	(% dQ 0.50)
Nitrate-rich	Levoglucosan	Set to zero	0
Nitrate-rich	Mannosan	Set to zero	0
Mineral dust	Ti	Pull up maximally	(% dQ 0.50)
Primary traffic	Levoglucosan	Set to 0	0
Primary traffic	Mannosan	Set to 0	0
Primary traffic*	Cu	Pull up maximally	(% dQ 0.50)

Primary traffic*	Fe	Pull up maximally	(% dQ 0.50)
Primary traffic*	Sn	Pull up maximally	(% dQ 0.50)
Primary traffic*	Ca ²⁺	Pull down maximally	(% dQ 0.50)
Primary traffic	Cu/Fe	Set to value	0.046 (% dQ 0.50)
Primary traffic	Cu/Sn	Set to value	5.6 (% dQ 0.50)
Primary traffic	Cu/Sb	Set to value	12.6 (% dQ 0.50)
Primary traffic	Cu/Mn	Set to value	5.7 (% dQ 0.50)
Primary traffic	OC*/EC	Set to value	0.44 (% dQ 0.50)

194 Note: *Only applied in Vif (peri-urban) site

195 **2.4.3 Criteria for a valid solution**

196 Solutions with a total number of factors between 7 and 12 were tested for the determination of the base cases. During factor
 197 selection, the Q/Q_{exp} ratio (<1.5), the geochemical interpretation of the factors, the weighted residual distribution, and the
 198 total reconstructed mass were evaluated. Finally, the optimal solutions obtained for each urban site was subjected to error
 199 estimation to ensure stability and accuracy of the solutions, using displacement (DISP) and bootstrapping (BS) methods. The
 200 DISP analysis evaluates that no swapping had occurred in any of the factors. Solutions with >80 out of 100 BS mapped
 201 factors were considered appropriate solutions. The final retained optimal solutions after the application of constraints
 202 fulfilled the recommendations of the European guide on air pollution source apportionment with receptor models (Belis et
 203 al., 2014). The sensitivity of the solutions to the applied constraints was also carefully evaluated by comparison between the
 204 base and constrained cases. More information about the source apportionment methodology is provided in the SI.

205 **2.4.4 Similarity assessment**

206 A test of similarity between source profiles, based on their specific chemical relative mass composition at each site was
 207 performed by comparing the Pearson distance (PD) and standardized identity distance (SID) in order to evaluate the
 208 variability of the solutions across these different urban environments. The PD and SID were calculated using Eq. S4 (Belis et
 209 al., 2015). Source profiles with PD<0.4 and SID<1.0 were regarded as similar (Pernigotti and Belis, 2018).

210 **2.4.5 Estimation of the contribution uncertainties**

211 The BS profiles uncertainties for the obtained solutions are presented in the SI (S3), in the form of mean±std of the 100 BS
 212 for all sites. As PMF5.0 does not directly output this to the user, we provided an estimate of the contribution uncertainties
 213 based on the method presented in Weber et al. (2019). During the BS estimation, both the G and F matrices are available,
 214 however only the F matrix is given back to the user (the G matrix being used internally to map the different profiles). Hence,
 215 the daily contributions of each of the species are estimated using:

216
$$X_{BSi} = G_{ref} \times F_{BSi}$$

217 where F_{BSi} is the profile of the bootstrap i, and X_{BSi} is the time series of each species according the reference contribution G_{ref}
218 and the bootstrap run F_{BSi} . Similarly, the DISP contribution uncertainties are given by the reference contribution G multiplied
219 by the lower and upper limits of the DISP result for each species.

220 **3 Results and discussion**

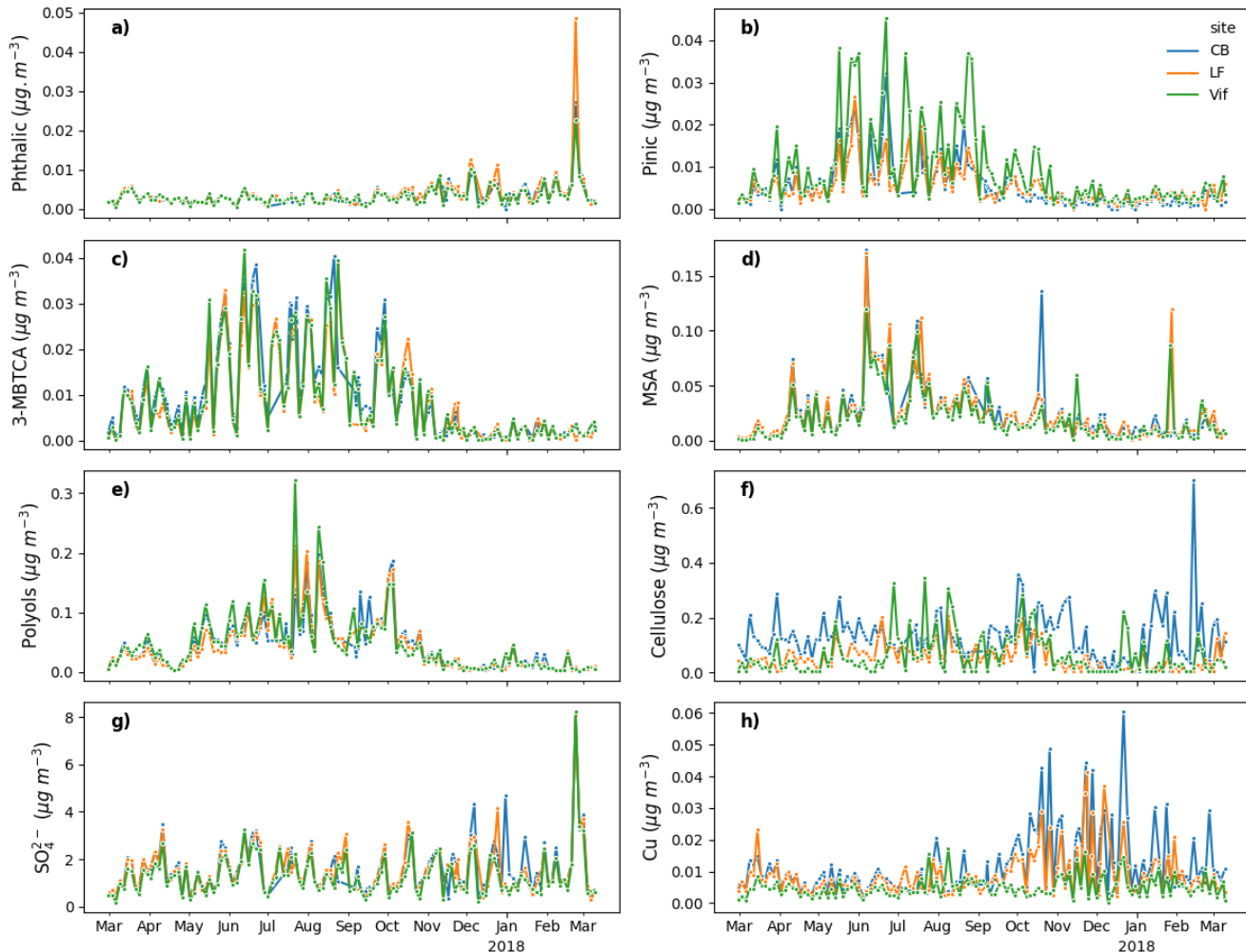
221 **3.1 General evolution of concentrations of PM₁₀ and chemical species**

222 The daily PM₁₀ mass concentrations at the three measurement sites determined with the TEOM FDMS for the dates of filter
223 sampling ranged from 3–61 µg m⁻³ with an overall average of 14±9 µg m⁻³ during the sampling period. Average PM₁₀ levels
224 were the highest at the urban hyper-center site (CB) (16±10 µg m⁻³), followed by the urban background site (LF) (14±8
225 µg m⁻³), and the peri-urban site (Vif) (13±9 µg m⁻³). Annual averages of PM₁₀ mass concentrations and chemical
226 compositions at all sites and at individual urban sites are shown in Table S2 in SI. The sites in this study showed minimal
227 exceedances of the current PM₁₀ European limit value of 40 µg m⁻³ (3.7%, 1.6%, and 1.6% of measurement days at the LF,
228 CB, and Vif sites, respectively). Most of these exceedances occurred during the winter season indicating the necessity to
229 additionally implement season-specific regulations for PM₁₀ emission reductions. Organic matter (OM) was the largest
230 contributor in PM₁₀ and accounted for 54%, 51%, and 56% of mass concentration on an annual basis in LF, CB, and Vif,
231 respectively. This contribution was followed by contributions from the major inorganic species (NH₄⁺, NO₃⁻, and SO₄²⁻),
232 suggesting strong influence from long-range transport of pollutants. An extensive description of the PM₁₀ chemistry in the
233 Grenoble basin has already been presented in Srivastava et al. (2018b) for the years 2013–2014 at the LF site. Our results
234 showed notable similarities for most chemical species for the year 2017–2018, especially in terms of seasonal variations and
235 respective contribution of chemical species to PM₁₀ mass concentrations. Therefore, we will only describe these aspects
236 briefly in this paper.

237 First, the time series analysis of PM₁₀ and its chemical composition in the Grenoble basin during the sampling period showed
238 mild to strong seasonal trends. Part of it can be attributed to the atmospheric dynamics in the area given its alpine
239 environment resulting in atmospheric temperature inversions that are especially common in winter. In the absence of strong
240 winds during the winter season (especially during anti-cyclonic periods), higher concentrations of air pollutants could be
241 expected. Indeed, PM₁₀ concentrations were higher during the colder months (October to April) with an average of 17±10
242 µg m⁻³ and lower during the warmer months (May to September) with an average of 10±4 µg m⁻³. We observed a strong
243 seasonality for some chemical species with higher concentrations during the colder months including OC*, EC, K⁺, NO₃⁻,
244 NH₄⁺, levoglucosan, mannosan, and phthalic acid. These species are commonly associated with primary emissions during the
245 process of biomass burning (OC, EC, K⁺, levoglucosan, mannosan) and secondary atmospheric processing (NO₃⁻, NH₄⁺,
246 phthalic acid). Alternatively, specific species with higher concentrations during warmer months include MSA, polyols, 3-
247 MBTCA, and pinic acid. These species are known to be products of a wide range of photochemical reactions in the
248 atmosphere partly formed by OH-initiated oxidation (Atkinson and Arey, 1998; Szmigielski et al., 2007) and can be

249 explained by enhanced photochemical production due to an increase of temperature-dependent hydroxyl radical (OH)
250 concentration. A summary of temporal evolutions of the concentration for some species including SO_4^{2-} , Cu, cellulose,
251 polyols, 3-MBTCA, pinic acid, and phthalic acid is shown in Figure 2.

252



253

254 **Figure 2: Temporal evolutions of a) phthalic acid, b) pinic acid, c) 3-MBTCA, d) MSA, e) polyols (arabitol+mannitol), f) cellulose,**

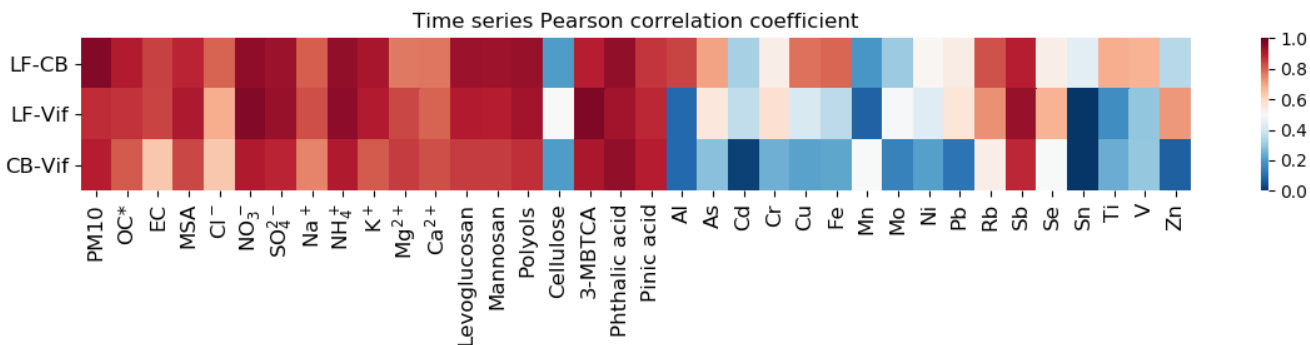
255 g) SO_4^{2-} and h) Cu in the three urban sites in the Grenoble basin (LF in orange, CB in blue, and Vif in green).

256

257 Second, the Pearson correlation coefficients of the temporal evolution of each species across sites is presented in Figure 3.
258 Similarity of temporal trends and strong correlations of PM_{10} components between our 3 sites indicates the influence of large
259 scale transport processes or possible uniform distribution of some emission sources in the Grenoble area. Further, the
260 accumulation and removal processes of the PM may be driven by similar season-specific environmental conditions at a local

scale. A strong correlation was observed in OC*, EC, ions, polyols, levoglucosan, mannosan, 3-MBTCA, phthalic acid, and pinic acid between sites suggesting similar origins and atmospheric processes affecting the concentrations of these species. The three sites seem to be equally impacted by long range transport since concentration of SO₄²⁻ appears almost identical. We also clearly see relatively similar temporal trends for the organic acids (MSA, pinic, and 3-MBTCA). Notably, we also observed an important episode in phthalic acid in late February 2018 affecting all the three sites. Conversely, cellulose and most metal species showed weak to mild correlations between sites, possibly indicating that the sources of these species are highly localized, with a potential impact that is variable at a city-scale. Particularly, cellulose presents similar order of magnitude at the three sites but presents higher concentration at CB, especially during winter. A few metals only showed strong correlations between LF and CB, but not with Vif, such as Al, Cu, Fe, Rb, and Sb which are tracers of road transport activity or biomass burning emissions. Specifically, Cu concentrations are similar at the three sites during summer, but presents significantly lower concentration in Vif compared to the two urban sites of CB and LF during winter.

272



273

274 **Figure 3: Heat map of the time series Pearson correlation coefficient of PM₁₀ and its chemical composition between LF and CB**
275 **(LF-CB), LF and Vif (LF-Vif), and CB and Vif (CB-Vif).**

276

277 **3.2 PM₁₀ source apportionment**

278 In the following sections, a description of the best PMF solution obtained after application of constrains is provided for each
279 of the 3 sites, together with a discussion about the factors that are associated with the added organic tracers (MSA, polyols,
280 cellulose, pinic and 3-MBTCA acids). The presentation of error estimations, chemical profiles, and temporal evolutions of
281 the PMF-resolved sources, and the discussion about the more classical factors can be found in the SI (S3).

282 **3.2.1 General description of the solutions**

283 The PMF model was applied independently on the data set of each three sites, using 35 chemical atmospheric compounds in
284 each site. The constrained solutions for each site consists of 11 factors, including common factors such as primary traffic,
285 biomass burning, nitrate-rich, sulfate-rich, aged sea salt, sea/road salt, and mineral dust. Also, with the use of biogenic tracer

21

22

286 species, we identified a primary biogenic factor and a MSA-rich factor, similar to Weber et al. (2019). We also determined a
287 metals-rich factor, identified as an industrial factor, accounting for a very small part of the PM₁₀ mass. Finally, using new
288 organic proxies (pinic and 3-MBTCA acids), we identified a secondary biogenic oxidation factor that is rarely described in
289 other PMF studies. Table 2 shows a synthesis of the tracers used to identify these 11 PMF-resolved factors that are found at
290 each of the 3 sites.

291 Other solutions with fewer or greater number of factors were also investigated but these solutions were less defined, and
292 factor merging was often observed. The reconstructed PM₁₀ contributions from all sources with measured PM₁₀ concentration
293 showed very good mass closure in all sites (LF: r=0.99, n=125, p<0.05; CB: r=0.99, n=126, p<0.05; and Vif: r=0.99, n=126,
294 p<0.05) indicating good model results.

295 This result is in line with a previous study in the city of Grenoble (Srivastava et al., 2018b), but with slight improvements in
296 the PM₁₀ mass closure (from r=0.93 to r=0.99). A complete comparison of the PMF-resolved sources between the two
297 studies is presented and discussed in SI (S4). The two sets of results are in good agreement, despite the samples being
298 collected 4 years apart. There were several identified sources that are similar in both studies such as biomass burning,
299 primary traffic, mineral dust, aged sea salt, sulfate- and nitrate-rich (identified collectively as secondary inorganics in
300 Srivastava et al. (2018b)), and primary biogenic (identified as fungal spores and plant debris in Srivastava et al. (2018b)).
301 Additionally, due to a number of differences in the input variables used, there are some sources that are completely unique to
302 each study. In particular, the sources that we have uniquely identified are industrial, sea/road salt, MSA-rich, and secondary
303 biogenic oxidation sources. Conversely, Srivastava et al., (2018b) have uniquely identified two SOA sources: biogenic SOA
304 and anthropogenic SOA. It can be argued that the secondary biogenic oxidation source (11%) in our study and the biogenic
305 SOA (12%) in Srivastava et al. (2018b) are in some way similar, although different tracers were used to identify them.
306 Lastly, while not uniquely identified in our study, the contributions of phthalic acid in several common anthropogenic-
307 derived sources (sulfate- and nitrate-rich) can also mark the potential contributions from anthropogenic SOA sources.
308 It is also important to note that, although still in the acceptable range, the sulfate-rich factor obtained in our PMF results
309 yielded the most BS unmapped factors amongst the PMF-resolved factors (up to 25% for the CB site). This could imply that
310 the sulfate-rich factor could potentially be susceptible to random errors and the effects of rotational ambiguity, and may be
311 the sign of possible mixing of different processes / sources.

312
313 **Table 2: Summary of PMF-resolved sources and their specific tracers.**

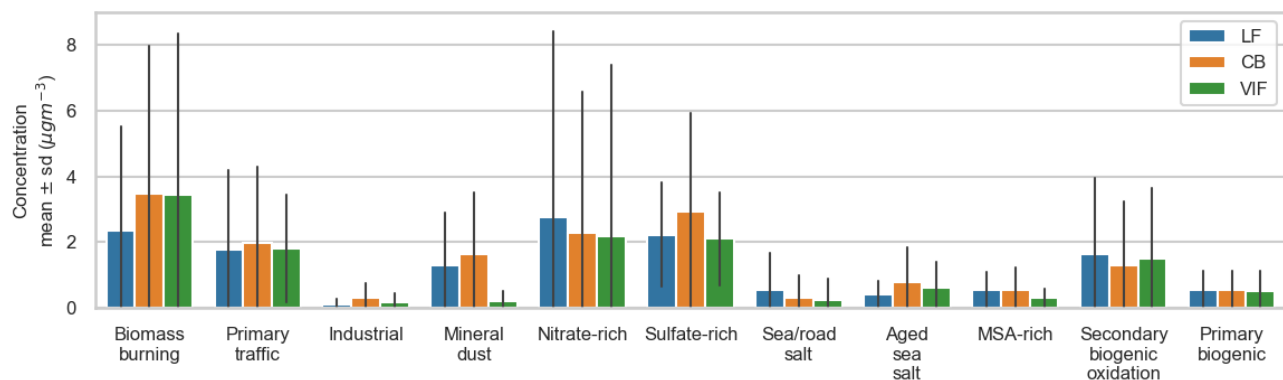
Identified factors	Specific tracers
Biomass burning	Levoglucosan, mannosan, K ⁺ , Rb, Cl ⁻
Primary traffic	EC, Ca ²⁺ , Cu, Fe, Sb, Sn
Nitrate-rich	NO ₃ ⁻ , NH ₄ ⁺ , phthalic acid
Sulfate-rich	SO ₄ ²⁻ , NH ₄ ⁺ , Se, phthalic acid
Mineral dust	Ca ^{2+*} , Al, Ti, V
Sea/road salt	Na ⁺ , Cl ⁻
Aged sea salt	Na ⁺ , Mg ²⁺

Industrial	As, Cd, Cr, Mn, Mo, Ni, Pb, Zn
Primary biogenic	Polyols, cellulose
MSA-rich	MSA
Secondary biogenic oxidation	3-MBTCA, pinic acid

314 Note: *Vif site did not have high loadings of Ca^{2+} specie in this factor

315 3.2.2 PM_{10} contribution

316 Biomass burning (17-26%), sulfate-rich (16-18%), and nitrate-rich (14-17%) sources were the highest contributors to the
 317 total PM_{10} mass on a yearly average in the Grenoble basin. Primary traffic (12-14%) and secondary biogenic oxidation (8-
 318 11%) sources also contributed a relevant amount. Figure 4 presents a comparison of the source contributions in each site
 319 based on mass concentration (in $\mu\text{g m}^{-3}$). These results are in line with recent studies leading to anthropogenic and SOA
 320 sources heavily influencing urban air pollution in western Europe (Daellenbach et al., 2019; Golly et al., 2019; Pandolfi et
 321 al., 2020; Srivastava et al., 2018b; Weber et al., 2019). The most notable difference across all sites is the sharp decrease of
 322 mineral dust in Vif compared to the other two urban sites, and this is discussed further in section 3.4.1.



323
 324 **Figure 4: Factor contributions in $\mu\text{g m}^{-3}$ for the three sites (LF: blue, CB: orange, Vif: green). Bar plots depict the mean annual**
 325 **value and the standard deviation of daily variations.**

326

327 3.2.3 MSA-rich

328 This factor is identified with a high loading of MSA, a known product of oxidation of dimethylsulfide (DMS), commonly
 329 described as resulting from marine phytoplankton emissions (Chen et al., 2018; Li et al., 1993). Other chemical species with
 330 significant concentrations in this factor include sulfate and ammonium. Although a very useful tracer of marine biogenic
 331 sources, MSA showed in our series only weak to mild correlations with ionic species from marine aerosols such as Na^+ (r :
 332 0.2–0.3) and Mg^{2+} (r : 0.3–0.4). This suggests potential emissions originating from terrestrial biogenic sources instead, which
 333 has been similarly suggested before (Bozzetti et al., 2017; Golly et al., 2019), and/or from forest biota (Jardine et al., 2015;
 334 Miyazaki et al., 2012). On an annual scale, this factor accounted for 2-4% of the total mass of PM_{10} and shows a strong

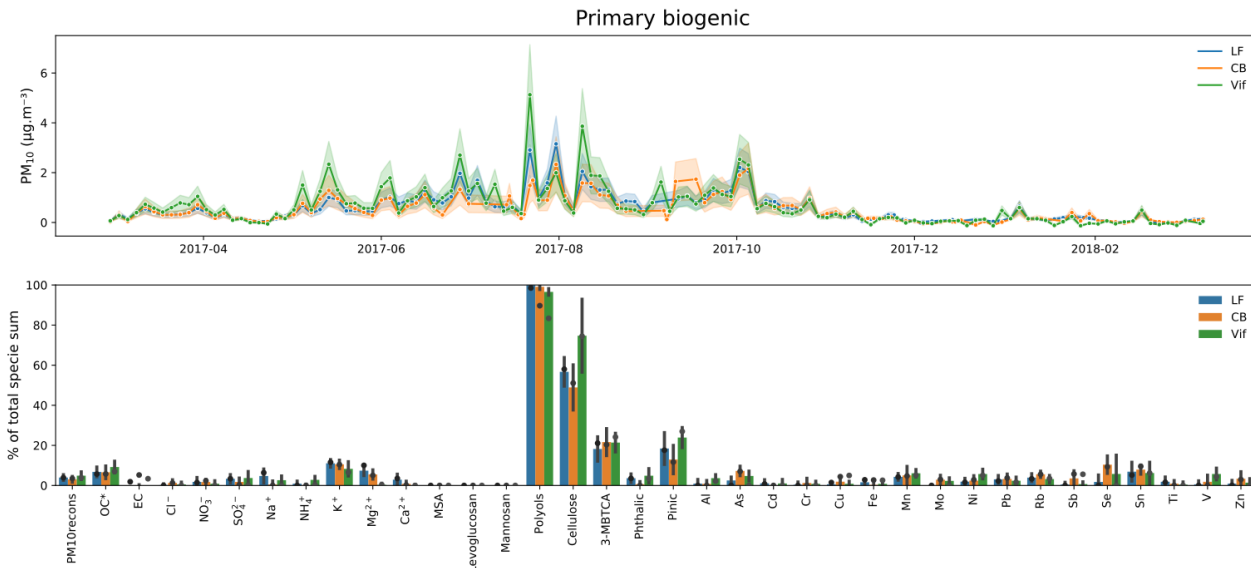
25
 26

335 seasonality with highest contributions during summer, reaching up to 53%, 57%, 52% of the total PM₁₀ mass in some
 336 specific days in LF, CB, and Vif, respectively. The similarity in the temporal distribution across sites, as shown in Figure
 337 S3.8, especially the summer peaks, could be linked to the influence of long-range transport of pollutants in the MSA-rich
 338 factor.

339 **3.2.4 Primary biogenic**

340 The primary biogenic factor was identified with high loadings of both polyols and cellulose (see Figure 5). Polyols
 341 (represented by the sum of arabitol and mannitol) are known as tracers of primary biological aerosols from fungal spores and
 342 microbes (Bauer et al., 2002; Igarashi et al., 2019). Polyols has been used in several studies as a tracer of biogenic sources,
 343 contributing in France within a range of 5-9% of PM₁₀ on a yearly average (Samaké et al., 2019, 2019; Srivastava et al.,
 344 2018b; Waked et al., 2014; Weber et al., 2019). Cellulose is a potential macro-tracer for plant debris from leaf litter and seed
 345 production (Kunit and Puxbaum, 1996; Puxbaum, 2003) that is very rarely used in source apportionment studies as of today,
 346 while it can represent a large fraction of the PM mass in the coarse mode (up to 6% during the warm season in the Vif site)
 347 (Bozzetti et al., 2016).

348



349

350 **Figure 5: Primary biogenic factor for the 3 urban sites. Top: Contribution to PM₁₀ given the mean and standard deviation of the**
 351 **100 BS. Bottom: Percentage (%) of each specie apportioned by this factor (dots refer to the constrained run, bar plots refer to the**
 352 **mean and error bars refer to the standard deviation of the 100 BS).**

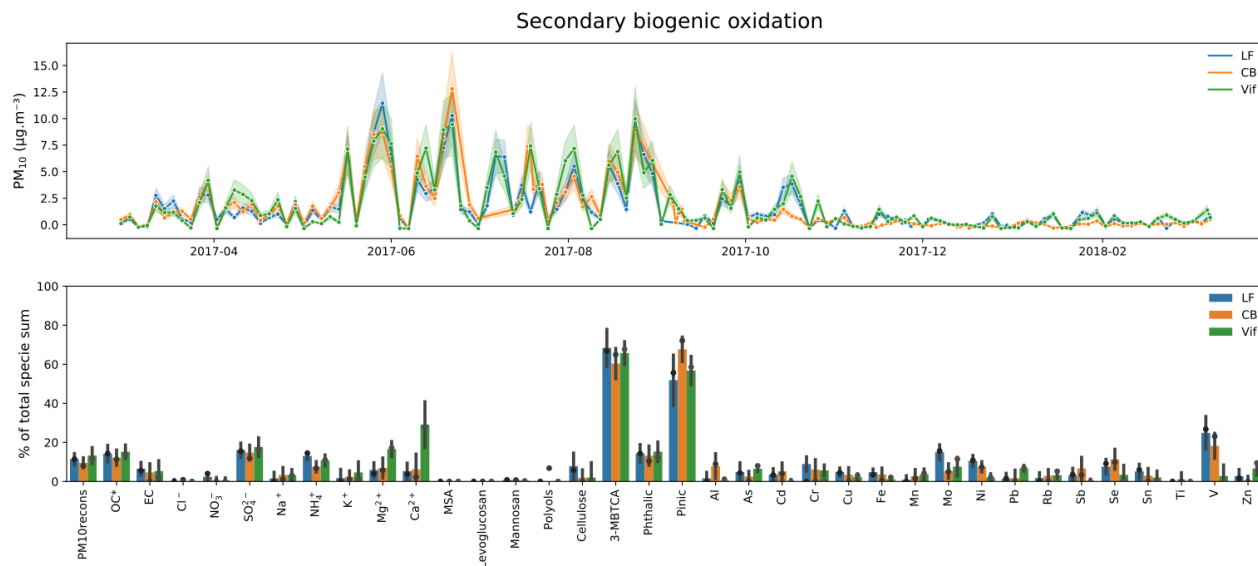
353

354 A strong correlation was found in the temporal evolution of polyols across the 3 sites in our study indicative of large scale
 355 impact of sources for these species (Samaké et al., 2019a,b). Conversely, cellulose concentrations present only weak

356 correlations across the 3 sites, possibly indicating that the influence of the sources of this specie might be more local.
 357 Although polyols and cellulose are both tracers of biogenic sources, only a rather mild correlation ($r=0.5$) was found
 358 between these two tracers, with seasonality of their concentrations being slightly different (Figure 2). It shows that the
 359 processes and the sources are probably distinct for the two sets of chemical species. However, the PMF is not able to
 360 separate them, and this factor includes most of the cellulose (58, 51, and 74 % in LF, CB, and Vif, respectively), and also
 361 most of the polyols (99, 90, and 83 % in LF, CB, and Vif, respectively). The remaining fraction of cellulose concentrations
 362 was included in the mineral dust factor in LF and CB, and in the primary traffic factor in Vif, suggesting the possibility of
 363 resuspension processes for this compound (see the SI for details). We can also note that the cellulose was not apportioned in
 364 the biomass burning factor, an indication that it may not be emitted by this source.

365 Despite their slightly different origins, the PMF analysis captures the combined contribution of polyols and cellulose to a
 366 factor that can be termed “primary biogenic sources”. In this study, this factor accounted for 3-4% of the total mass of PM_{10}
 367 on an annual scale, and a strong seasonality was observed, with up to 18% (in LF), 8% (in CB), and 17% (in Vif) of the total
 368 PM_{10} mass on average in summer, with specific days reaching up to 60% of PM_{10} for example at the Vif site (see Figure 5).
 369 These temporal variations are consistent with higher biological activity (increased production of fungal and fern spores, and
 370 pollen grains) in this season due to increase in temperature and humidity (Graham et al., 2003; Verma et al., 2018). This may
 371 also be attributed to an increased plant metabolic activity (production of plant debris from decomposition of leaves) and the
 372 proximity to forested and agricultural areas of the sampling sites (Gelencsér et al., 2007; Puxbaum, 2003).

373



374

375 **Figure 6: Secondary biogenic oxidation factor for the 3 urban sites.** Top: Contribution to PM_{10} given the mean and standard
 376 deviation of the 100 BS. Bottom: Percentage (%) of each specie apportioned by this factor (dots refer to the constrained run, bar
 377 plots refer to the mean and error bars refer to the standard deviation of the 100 BS).

379 **3.2.5 Secondary biogenic oxidation**

380 The secondary biogenic oxidation factor was identified with high loadings of 3-MBTCA and pinic acids (see Figure 6). Both
 381 tracers of this factor are known to be products of secondary oxidation processes of alpha-pinene from various biogenic
 382 origins. The apportionment of such a factor is not commonly achieved in receptor modelling using off-line tracers (van
 383 Drooge and Grimalt, 2015; Heo et al., 2013; Hu et al., 2010; Srivastava et al., 2018a). On an annual scale, this factor
 384 accounted for 8-11% of the total mass of PM₁₀, but can be as high as 58% (11 µg m⁻³) on specific days (see Figure 6, Top).
 385 The strong correlation between 3-MBTCA and pinic acids suggests similarity of origin of the secondary biogenic oxidation
 386 factor in the Grenoble area, despite inter-site correlations for 3-MBTCA (older oxidation state of alpha-pinene, hence more
 387 homogeneous at the city scale) being larger than that for pinic acid (former oxidation product, less homogeneous). Although
 388 significant portions (56-72%) of these species (3-MBTCA and pinic acids) are in this secondary biogenic oxidation factor,
 389 there are still relevant contributions in other factors, including primary biogenic, sulfate- and nitrate-rich, aged sea salt, and
 390 MSA-rich. Conversely, the presence of phthalic acid contribution in this factor (around 10% of its concentration), which
 391 could be emitted directly from biomass burning or formed during secondary processing from anthropogenic emissions
 392 (Hyder et al., 2012; Kleindienst et al., 2007; Wang et al., 2017b; Yang et al., 2016), also suggests that the secondary biogenic
 393 oxidation factor may be affected by these emissions. All of these indicate that the PMF process did not deliver a pure
 394 secondary biogenic oxidation factor, either due to data processing limitation or because of real mixing of these sources in the
 395 PM.

396

397 **3.3 Re-assignment of factors thanks to the new proxies**398 **3.3.1 Importance of the new proxy for factor identification**

399 With the use of these additional organic tracers, there are several added information drawn from the results of the PMF
 400 model. First, the notable contributions of phthalic acid in several sources could further confirm the mixing influence of
 401 anthropogenic processes in various sources of PM₁₀ such as sulfate- and nitrate-rich, but also with secondary biogenic
 402 oxidation sources. Second, adding 3-MBTCA and pinic acids in the input variables allowed the identification of a significant
 403 secondary biogenic oxidation factor that is generally difficult to identify with PMF studies of off-line samples. Comparisons
 404 already started with the factors obtained by AMS studies (Vlachou et al., 2018), but more work remain to be done in order to
 405 evaluate their proper correspondence.

406 **3.3.2 Comparison with a “classic” PMF solution**

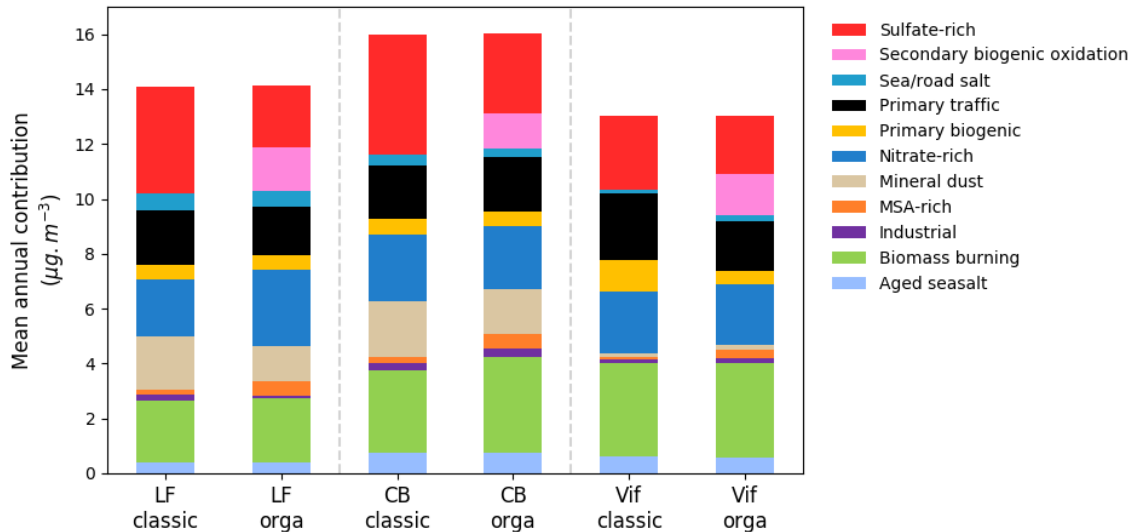
407 In order to quantify the added value and the changes brought in by the additional tracers, a reference PMF using a chemical
 408 data set (not including cellulose, pinic acid, phthalic acid, and 3-MBTCA) and parameters similar to that in the SOURCES

409 project (Weber et al., 2019) was performed, hereafter called “classic”, and the results were compared with those from the
410 present study (called “orga”). Figure 7 shows the comparison of the yearly average mass contribution of the different factors
411 for these two approaches. A detailed comparison of chemical profiles between the “classic” and “orga” PMF runs in each
412 site is summarized in the SI (S3). One can see that most observations below are consistent in all three sites.

413 Some factors remain unaffected or only marginally modified: it is the case for the biomass burning source with a percentage
414 increase in contribution, only ranging from 1-14%, in the “orga” compared to the “classic” PMF run across all sites. The
415 primary biogenic source also posed an interesting case with a minimal decrease in contribution at 0.1 and 6% in the LF and
416 CB sites, respectively. However, adding more specific biogenic tracers changed the contribution of the primary biogenic
417 factor in Vif, from $1.1 \mu\text{g m}^{-3}$ for the “classic” PMF down to $0.50 \mu\text{g m}^{-3}$ for the “orga” PMF run, a value that is much more
418 in line with the contributions observed at the other sites (0.56 and $0.55 \mu\text{g m}^{-3}$ in CB and LF, respectively). This further
419 highlights the usefulness of the additional organic tracers (e.g., addition of cellulose in the primary biogenic factor),
420 especially for specific site typologies.

421 Conversely, the most impacted factor is the sulfate-rich one, to a similar extent for the 3 sites with much higher mass fraction
422 in the “classic” PMF run in large part due to higher loadings of OC*. It may indicate possible merging with organic aerosol
423 sources in the “classic” PMF, as presented in a comparison of chemical profiles between the “classic” and “orga” PMF run
424 in each site summarized in the SI (S3). Figure 7 shows that the differences are really close to the content of the new
425 secondary biogenic oxidation factor. Secondary aerosols, such as the sulfate-rich factor, can be transported over long
426 distances and can remain in the atmosphere for about a week (Warneck, 2000), allowing them to interact with numerous
427 other species and undergo different atmospheric oxidation processes. In fact, several studies have investigated various
428 oxidation pathways of sulfate-rich sources (Barker et al., 2019; Ishizuka et al., 2000; Schneider et al., 2001; Ullerstam et al.,
429 2002, 2003; Usher et al., 2002). In the SPECIEUROPE database, several studies have reported sulfate-rich sources
430 influenced by a variety of different fuel combustion sources (Bove et al., 2014; Pernigotti et al., 2016; Pey et al., 2013). It is,
431 therefore, not surprising that part of the matter in the sulfate-rich source was re-assigned to different other sources upon
432 addition of the organic tracers in the “orga” PMF run. A comparable study in Metz (France) also used another organic tracer
433 (oxalate) to apportion a secondary organic aerosol (SOA) source from PM, ascribing it possibly to both biogenic and
434 anthropogenic emissions (Petit et al., 2019).

435



436

437 **Figure 7: Mean annual contribution ($\mu\text{g m}^{-3}$) of PMF-resolved factors of PM_{10} in the Grenoble basin using a classic set of input
438 variables similar to SOURCES (“classic”) and using additional new organic tracers (“orga”).**

439

440 We also observed an increase in the contributions of the MSA-rich factor at the three sites, with an increase in contributions
441 from specific inorganic species, such as SO_4^{2-} and NH_4^+ (see Figure S3.8.1 in the SI). Conversely, a decrease in contribution
442 from polyols was observed in the chemical profile of primary biogenic factor in Vif (see Figure S3.7.1 in the SI). Results
443 show that in the “classic” PMF run, the contribution of polyols was almost completely assigned to the primary biogenic
444 factor (>94% of its total mass) while the “orga” PMF run resulted in a contribution of polyols to the MSA-rich factor of
445 about 10% of its total mass.

446 Finally, there is also an observed re-assignment of the Ca^{2+} specie that further refined specific factors in Vif. The mineral
447 dust factor is often identified with high loadings of Ca^{2+} , however this is not the case for Vif, particularly for the “classic”
448 PMF run (less than 1% of total Ca^{2+} , although attached with important uncertainties). With the addition of the organic
449 tracers, there was an observed increase in the contribution of Ca^{2+} in the mineral dust factor in Vif (see Figure S3.11.1),
450 resulting to more than 20% of the total Ca^{2+} apportioned in this factor (a value is still attached with important uncertainties).
451 Interestingly, the contribution of Ca^{2+} is mainly transferred from the primary traffic factor to the mineral dust factor, resulting
452 in decreased contribution of the primary traffic factor in Vif from $2.4 \mu\text{g m}^{-3}$ for the “classic” PMF down to $1.8 \mu\text{g m}^{-3}$ for the
453 “orga” PMF run, again to a value closer to the contributions at the other sites (2.0 and $1.8 \mu\text{g m}^{-3}$ in CB and LF, respectively)
454 (see Figure S3.2.1 in the SI).

455 **3.3.3 Decrease of uncertainties**

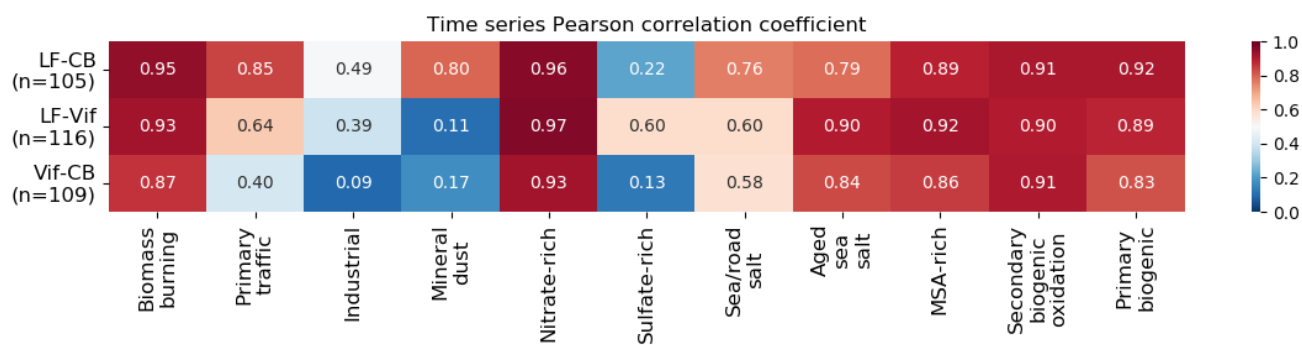
456 Another advantage of adding specific proxies in the PMF is the lowering of uncertainties associated with some other
 457 chemical species in some factors. Indeed, we observed a decrease of the BS uncertainties, notably for the OC* and also for
 458 some main tracers of sources in several profiles (see in the SI (S3)). The sulfate-rich is the most impacted factor when adding
 459 the new organic tracers and the higher uncertainties in the “classic” PMF run provided insights that this profile may have
 460 some internal mixing. Splitting this factor, thanks to the new organics, refined the sulfate-rich factor and strengthened the BS
 461 stability of this factor, decreasing the BS uncertainties.

462 Concerning the DISP, the range of uncertainties was also narrowed for 74% of the species in factors when comparing the
 463 “classic” and “orga” PMF. This decrease of uncertainties for the DISP when adding new variables was already observed by
 464 (Emami and Hopke, 2017), but our study additionally observe this in the BS error estimation. Overall, on top of being able to
 465 identify new factors, the addition of the new specific proxies in the PMF strengthened the confidence we have for all other
 466 factors.

467 **3.4 Fine scale variability of the temporal contribution**

468 Figure 3 indicates correlations of the concentrations for many chemical species across the sites. Additionally, the temporal
 469 evolution of the contribution of commonly resolved factors are further investigated in this section. Figure 8 presents the
 470 Pearson correlation coefficient of the contributions of the sources for the three pairs of sites. The sources that resulted to
 471 consistent strong correlations ($r>0.77$) across all sites are biomass burning, nitrate-rich, aged sea salt, MSA-rich, secondary
 472 biogenic oxidation, and primary biogenic sources. The sea/road salt factor showed good correlations across the sites with a
 473 correlation coefficient ranging from 0.58 to 0.76.

474



475

476 **Figure 8: Heat map of the time series Pearson correlation coefficient of all factor contributions between LF and CB (LF-CB), LF**
 477 **and Vif (LF-Vif), and CB and Vif (CB-Vif).**

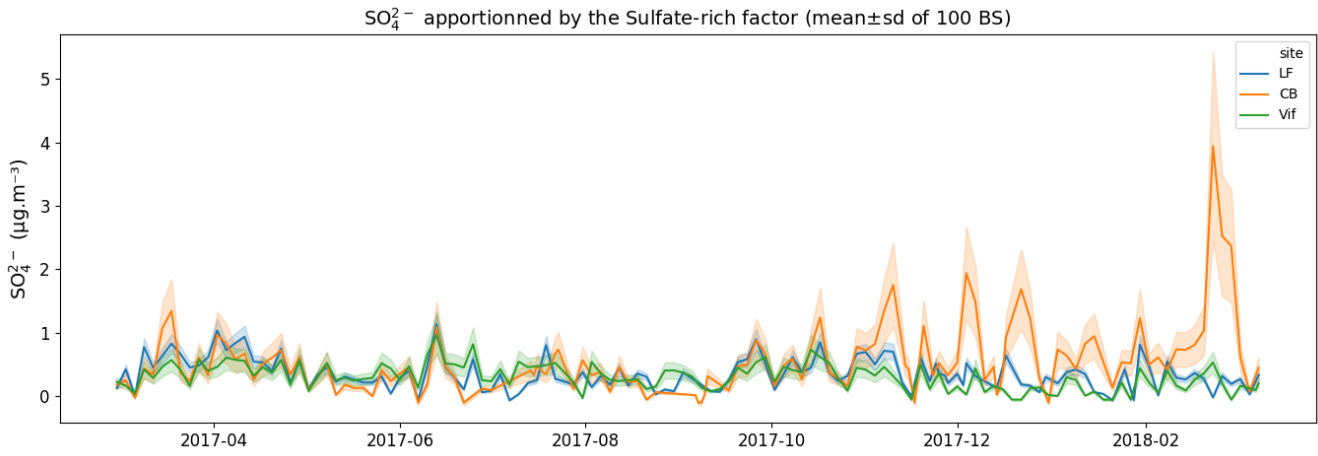
478

479 Factors with strong seasonality appeared to be highly correlated between sites (biomass burning, nitrate-rich, MSA-rich, and
480 primary biogenic). This tends to affirm that such factors are dominated either by large scale transport (i.e., nitrate-rich) or by
481 a strong climatic determinant. It is interesting to note that the primary biogenic factor presents systematically a slightly lower
482 correlation than the polyols (LF-CB: $r_{polyols}=0.94$ to $r_{primary\ biogenic}=0.91$, LF-Vif: $r_{polyols}=0.92$ to $r_{primary\ biogenic}=0.88$ and Vif-CB:
483 $r_{polyols}=0.87$ to $r_{primary\ biogenic}=0.82$). This may suggest a secondary process or a combination of several different primary
484 processes in the primary biogenic factor affecting the sites at different rates (Petit et al., 2019; Samaké et al., 2019) with
485 agglomeration or condensation occurring on the organic part of the PM, hence varying the temporal contribution of this
486 factor. We also clearly see a stronger similarity between LF and CB rather than Vif and the other two sites, notably for the
487 primary traffic, mineral dust, and to a lower extent the industrial factor. This may be explained not only by the proximity of
488 the location of the two former sites within the city, but also by their similarity in typology compared to the peri-urban site
489 type in Vif. However, there are two factors that do not present good correlation between all sites.

490 One of them is the sulfate-rich factor which presents a similar contribution when comparing LF and Vif, but low-to-none
491 correlation when compared to CB. A deeper analysis shows that the sulfate-rich, together with the nitrate-rich factor in CB,
492 explains a large part of the winter spike of secondary inorganics (23/02/2018 to 24/02/2018), whereas in LF and Vif only the
493 nitrate-rich factor explains most of it. This spike drives the Pearson correlation coefficient to a low value and without it, the
494 correlation increases drastically (see Figure S5.1 in the SI for the full scatterplot). Some PMF solutions of the BS in LF and
495 Vif also had this behaviour, but weren't chosen as the "best" solution. We propose two hypotheses for this difference: 1)
496 during winter, some heterogeneous chemistry may take place in fog episodes in the Grenoble basin (resulting to random
497 spikes in the SO_4^{2-} contribution), that may not be spatially homogeneous at the city scale, leading to mixing of secondary
498 sources, and 2) we have reached the limit of the PMF methodology to de-convolute further the secondary inorganics. Both
499 hypotheses may be concurrent.

500 We note however that apart from these spikes, the SO_4^{2-} apportioned by this factor at 3 sites are in good agreement, and are
501 within the uncertainties of each other (see Figure 9). This figure also highlights that the uncertainty for the SO_4^{2-} in this factor
502 is higher for the CB site, as also shown in the chemical profile in Figure S3.6 in the SI.

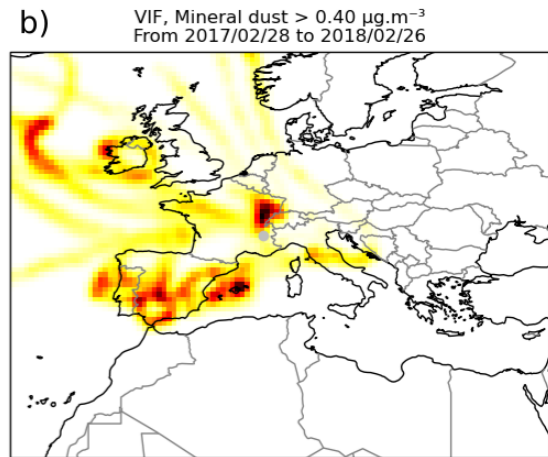
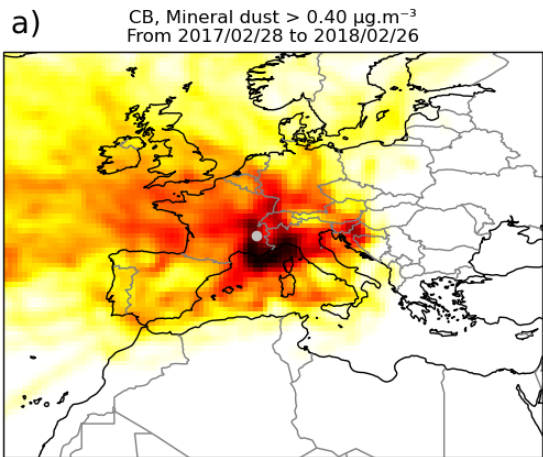
503



504
505 **Figure 9: SO_4^{2-} apportionned by the sulfate-rich factor at the 3 sites, according to the uncertainties given by the 100 BS as shown by**
506 **the mean (solid line) and the standard deviation (shaded area).**

507
508 The second factor which showed low correlations between pairs of sites is mineral dust, specifically when comparing Vif to
509 the two other sites. This is in line with the difference in the PM_{10} apportioned by this factor as shown in the previous section.
510 However, a closer look on the contribution scatterplot of $\text{Vif}_{\text{Mineral dust}}$ vs $\text{CB}_{\text{Mineral dust}}$ (see Figure S5.2 in the SI) highlights that
511 some events are very close to the 1:1 line. This is indicative of two regimes for mineral dust, with cases when the sources for
512 the urban and peri urban are being similar and cases when they are different. To investigate it further, a potential source
513 contribution function (PSCF) analysis of the mineral dust factor for the Vif and CB sites was performed in order to assess the
514 origin of air masses of this factor. It is presented in Figure 10. We can clearly see that for the Vif site, the main origin is
515 Spain, whereas the origin for CB is not well-defined. These PSCF pattern tends to indicate that the sources of the mineral
516 dust factor present a strong local component for the urban sites (CB and LF being very similar), while the origin of the
517 mineral dust factor in Vif appears to be mainly affected by long-range transport of dust only.

518



519

520 **Figure 10: The PSCF analysis of the days with a mineral dust loading higher than 0.4 $\mu\text{g m}^{-3}$ for the CB site (a) and Vif (b).**
 521 Darker shades indicate higher probability density of source origin.

522

523 3.5 Fine-scale variability of chemical profiles

524 An additional similarity test was also performed to investigate the fine-scale variabilities of the chemical profiles of the
 525 factors. A similarity analysis at a regional scale in France identified stable chemical profiles obtained by PMF studies across
 526 many sites, corresponding to biomass burning, sulfate-rich, nitrate-rich, and fresh sea salt factors (Weber et al., 2019). In our
 527 study, a parallel analysis was performed in order to evaluate the stability of the chemical profiles of the identified factors in
 528 high proximity receptor locations. Briefly, PMF-resolved sources were compared for each pair of sites using both Pearson
 529 distance (PD) and standardized identity distance (SID) to obtain a similarity metric (PD-SID). The PD metric represents the
 530 sensitivity of a chemical profile based on the differences in the major mass fractions of PM, whereas the SID represents the
 531 sensitivity to all components (hence taking into account trace species). Homogenous profiles that are stable over different
 532 site types are expected to have PD<0.4 and SID<1.0 (Pernigotti and Belis, 2018). Conversely, factors outside of this range
 533 are considered to have heterogeneous profiles.

534 3.5.1 (Dis-)similarity of the chemical profiles at the three sites

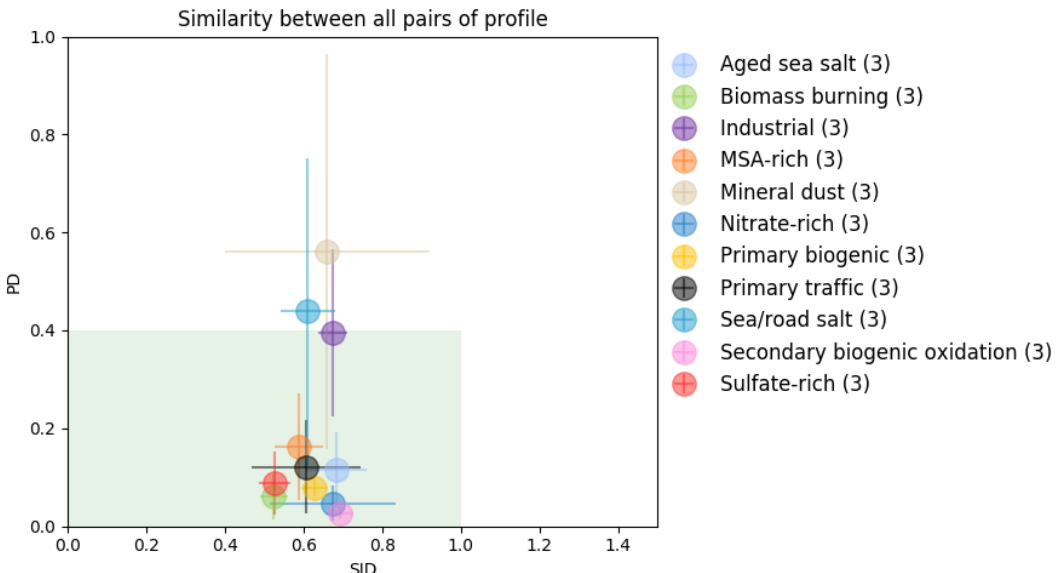
535 Figure 11 presents the similarity plot (PD-SID) obtained for the 11 factors found in this study. The biomass burning factor
 536 yielded the most stable chemical profile in all the sites in the Grenoble basin, which is consistent. Other stable factors
 537 include sulfate- and nitrate-rich, primary biogenic, MSA-rich, and secondary biogenic oxidation. The industrial and sea/road
 538 salt factors, both marginally above the accepted PD metric, could be considered as having heterogeneous profiles based on
 539 the contributions of these sources to the total PM_{10} in each site.

43

44

540 However, a clear heterogeneous chemical profile was found in the mineral dust, this further emphasized the difference in
 541 origin of this factor as previously discussed in section 3.4. More details about of the chemical profile of this factor can be
 542 found Figure S3.11 in the SI. One of the main difference is the lack of OC* in the Vif site compared to LF and CB sites,
 543 together with a much lower Ca²⁺ contribution. Additionally, there is a lower SO₄²⁻ apportioned in the mineral dust factor in
 544 Vif. The only similarity between all the sites are the high loadings of Al, Ti and V, as well as important contributions from
 545 other crustal metals (Fe, Ni, Mn). It also has to be noted that the cellulose is present up to about 20% of its total mass in the
 546 mineral dust profile in the CB site, however the BS estimates indicate very important uncertainties for this specie in this
 547 factor (see Figure S3.11 in the SI).

548



549

550 **Figure 11: Similarity plot of all chemical profiles in each site. The shaded area (in green) shows the acceptable range of the PD-
 551 SID metric. For each point, the error bars represent the standard deviation of the 3 pairs of comparisons.**

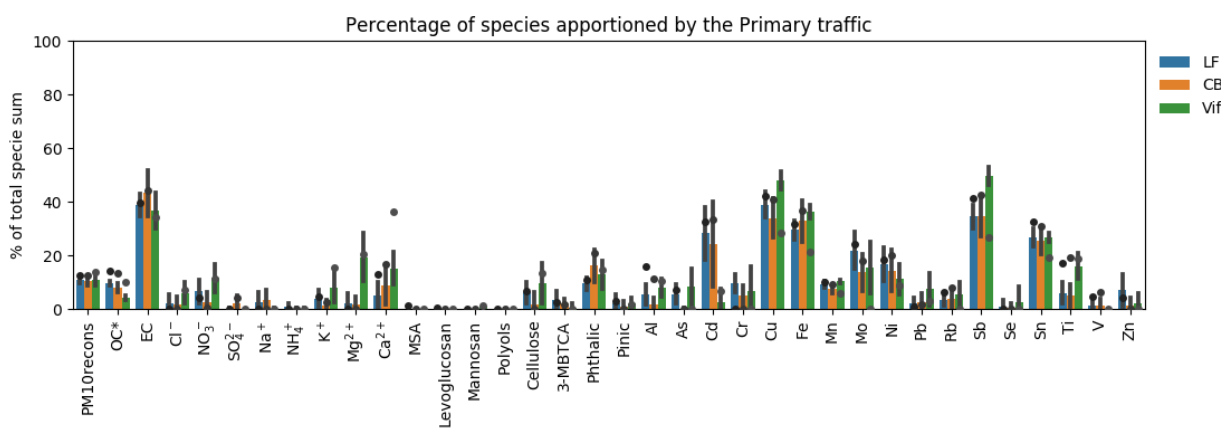
552

553 Surprisingly, the sulfate-rich factor chemistry is one of the most stable profile, although its temporal contributions exhibits
 554 high spatial variation, notably at CB compared to LF and Vif sites.

555 Finally, although the primary traffic factor showed a stable profile based on the similarity plot (PD-SID metric), it has to be
 556 noted that, in the reference run (i.e., constrained), the specie concentrations are within the BS uncertainties for all species at
 557 LF and CB sites, but outside the BS range for the Vif site (see Figure 12). Notably, the BS predicted higher contribution
 558 from Cu, Fe, Sb and Sn, which are common tracers of tyre and brake wear, than the reference run. Additionally, the Ca²⁺ is
 559 overestimated in the reference run by a large amount, as well as the OC*, and, to a lesser extent, the reconstructed PM₁₀.
 560 Such BS results indicate that, in Vif, the primary traffic factor is heavily influenced by this phenomenon on specific days,

45
46

561 that has led to an overestimation of the total PM₁₀ apportioned by this factor. Additionally, even at low concentrations, some
 562 terrestrial elements (Al, As, Ti) and cellulose are present in the primary traffic factor. As a result, even if the primary traffic
 563 characteristic of this factor is dominant, the influence of road dust re-suspension is not negligible for this factor in Vif.
 564



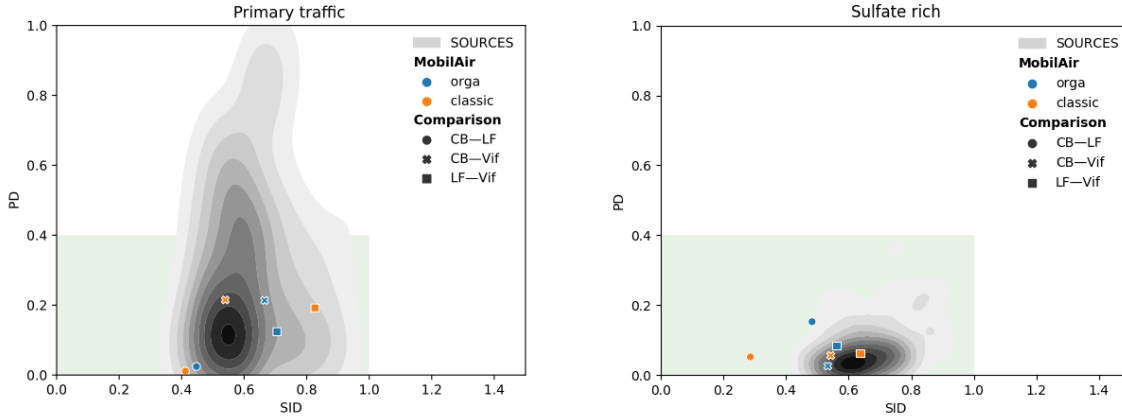
565
 566 **Figure 12: Percentage (%) of each species apportioned by the primary traffic factor (dots refer to the constrained run, bar plots
 567 refer to the mean and error bars refer to the standard deviation of the 100 BS).**

568
 569 **3.5.2. Comparison with other chemical profiles of PM₁₀ sources from a regional study**
 570 It is interesting to evaluate if a PMF study conducted at a city scale is leading to more similar source chemical profiles than a
 571 study using a database from a much larger area. Another question is whether PMF can produce more similar chemical source
 572 profiles with the help of additional organic tracers than a “classic” PMF run. Hence, the results obtained here are compared
 573 to those in the SOURCES program (Weber et al., 2019) for the 9 factors common in both studies (the secondary biogenic
 574 factor was not identified in the SOURCES program with the data sets not including its proper chemical tracers). This can be
 575 represented with the projection on a similarity plot of the distances between the factors for the 3 pairs of sites over the
 576 Grenoble basin, both for the “classic” and “orga” PMF. This is compared to the results from all possible pairs of sites within
 577 the 15 sites of the SOURCES study (distributed over France), mapped with a probability density function of similarities.
 578 Figure 13 presents these plots for the factors “primary traffic” and “sulfate-rich”, the other factors being presented in the SI
 579 (S6).

580 It shows that in most instances, the PMF results obtained for the Grenoble basin deliver slightly closer chemical profiles,
 581 both for the PD distance (sensitive to major components) and the SID distance (sensitive to the global profile), than the
 582 studies across more distant sites. This is particularly the case when comparing the two urban sites (LF and CB) (cf., Figure
 583 11). Some values out of the acceptable range remain for some factors (mineral dust, industrial), involving the differences
 584 between the urban and suburban sites, but are still fitting with the pattern obtained for the over-all French sites. The addition
 585 of the organic tracers did not alter the source profiles of the commonly resolved PMF factors and, in fact, even enhanced it

586 by further refining the other identified sources. This is predominantly seen in the MSA-rich factor, where some of the
587 “classic” PMF results fell outside the acceptable range while the “orga” PMF are all in the acceptable range of the similarity
588 plot. The “orga” PMF run for some factors such as primary biogenic, dust, and industrial factor also mostly yielded better
589 PD and SID metrics (closer to the acceptable range) than the “classic” PMF run.

590



591

592 **Figure 13: Similarity plots for the factor “Primary traffic” and “Sulfate-rich” for the pairs of sites formed in this study, compared**
593 **to the probability density function of similarities obtained for the 15 French sites of the SOURCES program.**

594

595 **3.6 Improvement of the identified sources with the new organic tracers**

596 In order to comprehensively apportion PM_{10} sources, the very large unknown portion of OM, especially in the secondary
597 fraction, needs to be properly identified. Most source apportionment studies only use standard input variables including OC,
598 EC, ions, and metals. However, these species alone are insufficient to describe the complexity of the organic matter, making
599 it a challenge to apportion sources from the OM fraction and their formation processes (i.e. primary or secondary origin)
600 (Srivastava et al., 2018a). Only a small number of studies have used organic tracers to apportion SOA in PM using PMF, and
601 even these studies usually have limited number of samples, number of tracers, and/or identified sources (Feng et al., 2013;
602 Shrivastava et al., 2007; Srivastava et al., 2018a). A few of these studies have proposed to estimate SOC contributions from
603 the sum of OC loadings in the secondary inorganic (nitrate- and sulfate-rich) factor (Hu et al., 2010; Ke et al., 2008; Lee et
604 al., 2008; Pachon et al., 2010; Yuan et al., 2006) or from water-soluble OC and humic-like substances (Qiao et al., 2018).
605 Some have estimated the contributions of biogenic SOA from the oxidation products of isoprene, alpha-pinene, and beta-
606 caryophyllene (Heo et al., 2013; Kleindienst et al., 2007; Miyazaki et al., 2012; Shrivastava et al., 2007; Wang et al., 2012).
607 In fact, the high contributions of biogenic SOA during warmer periods, that could range from 20-60% (Heo et al., 2013;
608 Miyazaki et al., 2012; Wang et al., 2012; Zhang et al., 2010), found by other PMF studies is also consistent with our
609 findings. Wang et al. (2017b) also highlighted the importance of biogenic SOA tracers as it significantly impacts the source

49
50

610 apportionment results, particularly in areas with strong SOA contributions. Although applied on a small sample size, an
611 interesting technique assimilating polar SOA tracers and primary organic aerosol (POA) tracers was performed by Hu et al.
612 (2010) resulting to two identified SOA factors that are mixed with: 1) secondary inorganics and biomass burning, 2) green
613 waste and biomass burning. Hence, with the appropriate uncertainties, the SOA tracers can be a practical way, possibly even
614 necessary, to estimate SOA contributions (Feng et al., 2013) especially in urban areas (Wang et al., 2012).
615 Our study demonstrated that the use of organic tracers aided an effective source-specific approach that clearly identified
616 major sources of SOA in PM₁₀ such as MSA-rich and secondary biogenic oxidation sources. The potential influence of
617 anthropogenic emissions on some sources was also observed through the contribution of one of the organic tracers used,
618 phthalic acid. The sufficient number of samples ($n>125$ for each site) in our study have also maintained the statistical
619 robustness of the solutions obtained from filter-based measurements. The stability of the organic tracers also resulted to
620 homogeneous chemical profiles which allowed seamless identification of uncommonly resolved sources such as primary
621 biogenic, secondary biogenic oxidation, and MSA-rich. Although the addition of cellulose did not emerge as a separate
622 biogenic factor, it provided an option to scrutinize the difference in terms origin of the primary biogenic sources across sites.
623 Overall, the organic tracers have further refined the contribution of other identified sources by taking in consideration the
624 SOA portion of PM₁₀ that would have otherwise mixed with other sources and have facilitated an innovative approach to
625 improve the apportionment of PM₁₀ sources.

626

627 **4 Conclusions**

628 A fine-scale source apportionment of PM₁₀ in different urban typologies (background, pedestrian hyper-center, and peri-
629 urban) in a small scale area (<15 km) was performed using PMF 5.0. Additional organic tracers (MSA, cellulose, 3-
630 MBTCA, pinic acid, and phthalic acid) were used to supplement the standard input variables. An 11-factor optimal solution
631 was found for each of the three urban sites, including primary traffic, nitrate-rich, sulfate-rich, industrial, biomass burning,
632 aged sea salt, sea/road salt, mineral dust, primary biogenic, secondary biogenic oxidation, and MSA-rich sources. The results
633 from previously reported PMF studies in Grenoble (Srivastava et al., 2018b; Weber et al., 2019) were confirmed by the
634 findings in this study particularly the long-term stability of regional source emissions over the last 5 years. The PMF solution
635 obtained with the additional organic tracers resulted to:

- 636 1. the improvement of PM₁₀ mass closure and the exploration of appropriate input variable uncertainties;
637 2. the re-assignment of the bulk sulfate-rich factor contribution to more descriptive secondary aerosol sources in the
638 atmosphere;
639 3. the clear identification of commonly unresolved sources in the SOA fraction (e.g., primary biogenic, traced by the
640 polyols and cellulose; secondary biogenic oxidation, traced by 3-MBTCA and pinic acid; and MSA-rich, traced by
641 the MSA) in different urban typologies;

51
52

642 4. the decreased uncertainties, for both BS and DISP error estimates, that further strengthened confidence in the PMF
643 solution;

644 5. the increased knowledge of the stability of the chemical profiles of the factors, that could be a key when using them
645 in further large-scale analysis or modeling;

646 The 3 sites comparison at a local scale:

647 6. highlights very similar profiles and temporal evolution in the factor contributions at a conurbation scale (such as the
648 Grenoble basin);

649 7. allows the determination of local heterogeneities in a small scale area and identification of some local hotspots;

650 8. pointed out some difficulties to disentangle the secondary inorganics sources (NO_3^- and SO_4^{2-}) and some mixing
651 between both species may occur.

652 Over-all, an enhanced and fine-scale source profile of PM_{10} was obtained in the Grenoble basin. The trend observed in the
653 MSA-rich, secondary biogenic oxidation, and primary biogenic factors showed the extent of this phenomenon suggesting
654 importance of the contribution of biogenic sources, both primary and secondary. The significant percentage attributed to
655 SOA sources revealed the strong necessity of organic molecular markers in fully discriminating the origins of PM_{10} sources.

656 **Acknowledgements**

657 This work is supported by the French National Research Agency in the framework of the "Investissements d'avenir"
658 program (ANR-15-IDEX-02), for the Mobil'Air program. It also received support from the program QAMECS funded by
659 ADEME (convention 1662C0029), and from LCSQA and French Ministry of Environment for part of the analyses for the
660 Les Frenes site within the CARA program. Chemical analysis on the Air-O-Sol facility at IGE was made possible with the
661 funding of some of the equipment by the Labex OSUG@2020 (ANR10 LABX56). The PhD of SW is funded by ENS Paris.
662 The internship of T Cañete is taking place within the Erasmus exchange program. Finally, the authors would like to kindly
663 thank the dedicated efforts of many people from Atmo-AuRA at the sampling sites, and in the lab at IGE (A Vella, C Vérin,
664 C Voiron) for collecting and analysing the samples, respectively.

665

666 **Authors contributions**

667 GU, and JLJ designed the atmospheric chemistry part of the Mobil'Air program. SM and CT supervised the sampling at the
668 3 sites for Atmo AuRA. OF is the head of the CARA program that allows the collection of samples from Les Frênes site. VJ
669 set up the analytical techniques for polyols, sugars, and cellulose. TC performed the cellulose analyses. LJSB and SW
670 processed the data. SW developed some of the tools and ideas for in-depth PMF analysis. LJSB, SW, wrote the paper. JLJ
671 and GU revised the original draft. All authors reviewed and edited the manuscript.

672 **References**

- 673 Alleman, L. Y., Lamaison, L., Perdrix, E., Robache, A. and Galloo, J.-C.: PM₁₀ metal concentrations and source
674 identification using positive matrix factorization and wind sectoring in a French industrial zone, *Atmospheric Research*,
675 96(4), 612–625, doi:10.1016/j.atmosres.2010.02.008, 2010.
- 676 Atkinson, R. and Arey, J.: Atmospheric Chemistry of Biogenic Organic Compounds, *Acc. Chem. Res.*, 31(9), 574–583,
677 doi:10.1021/ar970143z, 1998.
- 678 Aymoz, G., Jaffrezo, J. L., Chapuis, D., Cozic, J. and Maenhaut, W.: Seasonal variation of PM₁₀ main constituents in two
679 valleys of the French Alps. I: EC/OC fractions, *Atmos. Chem. Phys.*, 7(3), 661–675, doi:10.5194/acp-7-661-2007, 2007.
- 680 Barker, J. R., Steiner, A. L. and Wallington, T. J.: Advances in Atmospheric Chemistry: Volume 2: Organic Oxidation and
681 Multiphase Chemistry, WORLD SCIENTIFIC., 2019.
- 682 Belis, C. A., Favez, O., Harrison, R. M., Larsen, B. R., Amato, F., El Haddad, I., Hopke, P. K., Nava, S., Paatero, P., Prévôt,
683 A., Quass, U., Vecchi, R., Viana, M., European Commission, Joint Research Centre and Institute for Environment and
684 Sustainability: European guide on air pollution source apportionment with receptor models., Publications Office,
685 Luxembourg., 2014.
- 686 Belis, C. A., Pernigotti, D., Karagulian, F., Pirovano, G., Larsen, B. R., Gerboles, M. and Hopke, P. K.: A new methodology
687 to assess the performance and uncertainty of source apportionment models in intercomparison exercises, *Atmospheric
688 Environment*, 119, 35–44, doi:10.1016/j.atmosenv.2015.08.002, 2015.
- 689 Belis, C. A., Pikridas, M., Lucarelli, F., Petralia, E., Cavalli, F., Calzolai, G., Berico, M. and Sciare, J.: Source
690 apportionment of fine PM by combining high time resolution organic and inorganic chemical composition datasets,
691 *Atmospheric Environment: X*, 3, 100046, doi:10.1016/j.aeaoa.2019.100046, 2019.
- 692 Belis, C. A., Pernigotti, D., Pirovano, G., Favez, O., Jaffrezo, J. L., Kuenen, J., Denier van Der Gon, H., Reizer, M., Riffault,
693 V., Alleman, L. Y., Almeida, M., Amato, F., Angyal, A., Argyropoulos, G., Bande, S., Beslic, I., Besombes, J.-L., Bove, M.
694 C., Brotto, P., Calori, G., Cesari, D., Colombi, C., Contini, D., De Gennaro, G., Di Gilio, A., Diapouli, E., El Haddad, I.,
695 Elbern, H., Eleftheriadis, K., Ferreira, J., Vivanco, M. G., Gilardoni, S., Golly, B., Hellebust, S., Hopke, P. K., Izadmanesh,
696 Y., Jorquera, H., Krajsek, K., Kranenburg, R., Lazzeri, P., Lenartz, F., Lucarelli, F., Maciejewska, K., Manders, A.,
697 Manousakas, M., Masiol, M., Mircea, M., Mooibroek, D., Nava, S., Oliveira, D., Paglione, M., Pandolfi, M., Perrone, M.,
698 Petralia, E., Pietrodangelo, A., Pillon, S., Pokorna, P., Prati, P., Salameh, D., Samara, C., Samek, L., Saraga, D., Sauvage, S.,
699 Schaap, M., Scotto, F., Segà, K., Siour, G., Tauler, R., Valli, G., Vecchi, R., Venturini, E., Vestenius, M., Waked, A. and
700 Yubero, E.: Evaluation of receptor and chemical transport models for PM₁₀ source apportionment, *Atmospheric
701 Environment: X*, 5, 100053, doi:10.1016/j.aeaoa.2019.100053, 2020.
- 702 Birch, M. E. and Cary, R. A.: Elemental Carbon-Based Method for Monitoring Occupational Exposures to Particulate Diesel
703 Exhaust, *Aerosol Science and Technology*, 25(3), 221–241, doi:10.1080/02786829608965393, 1996.
- 704 Bove, M. C., Brotto, P., Cassola, F., Cuccia, E., Massabò, D., Mazzino, A., Piazzalunga, A. and Prati, P.: An integrated
705 PM_{2.5} source apportionment study: Positive Matrix Factorisation vs. the chemical transport model CAMx, *Atmospheric
706 Environment*, 94, 274–286, doi:10.1016/j.atmosenv.2014.05.039, 2014.
- 707 Bozzetti, C., Daellenbach, K. R., Hueglin, C., Fermo, P., Sciare, J., Kasper-Giebl, A., Mazar, Y., Abbaszade, G., El Kazzi,
708 M., Gonzalez, R., Shuster-Meiseles, T., Flasch, M., Wolf, R., Křepelová, A., Canonaco, F., Schnelle-Kreis, J., Slowik, J. G.,
709 Zimmermann, R., Rudich, Y., Baltensperger, U., El Haddad, I. and Prévôt, A. S. H.: Size-Resolved Identification,

- 710 Characterization, and Quantification of Primary Biological Organic Aerosol at a European Rural Site, Environ. Sci.
711 Technol., 50(7), 3425–3434, doi:10.1021/acs.est.5b05960, 2016.
- 712 Bozzetti, C., Sosedova, Y., Xiao, M., Daellenbach, K. R., Ulevicius, V., Dudoit, V., Mordas, G., Byčenkinė, S.,
713 Plauškaitė, K., Vlachou, A., Golly, B., Chazeau, B., Besombes, J.-L., Baltensperger, U., Jaffrezo, J.-L., Slowik, J. G., El
714 Haddad, I. and Prévôt, A. S. H.: Argon offline-AMS source apportionment of organic aerosol over yearly cycles for an
715 urban, rural, and marine site in northern Europe, Atmos. Chem. Phys., 17(1), 117–141, doi:10.5194/acp-17-117-2017, 2017.
- 716 Brunekreef, B.: Epidemiological evidence of effects of coarse airborne particles on health, European Respiratory Journal,
717 26(2), 309–318, doi:10.1183/09031936.05.00001805, 2005.
- 718 Bullock, K. R., Duvall, R. M., Norris, G. A., McDow, S. R. and Hays, M. D.: Evaluation of the CMB and PMF models using
719 organic molecular markers in fine particulate matter collected during the Pittsburgh Air Quality Study, Atmospheric
720 Environment, 42(29), 6897–6904, doi:10.1016/j.atmosenv.2008.05.011, 2008.
- 721 Cavalli, F., Viana, M., Yttri, K. E., Genberg, J. and Putaud, J.-P.: Toward a standardised thermal-optical protocol for
722 measuring atmospheric organic and elemental carbon: the EUSAAR protocol, Atmos. Meas. Tech., 3(1), 79–89,
723 doi:10.5194/amt-3-79-2010, 2010.
- 724 Charron, A., Polo-Rehn, L., Besombes, J.-L., Golly, B., Buisson, C., Chanut, H., Marchand, N., Guillaud, G. and Jaffrezo, J.-
725 L.: Identification and quantification of particulate tracers of exhaust and non-exhaust vehicle emissions, Atmos. Chem.
726 Phys., 19(7), 5187–5207, doi:10.5194/acp-19-5187-2019, 2019.
- 727 Chen, Q., Sherwen, T., Evans, M. and Alexander, B.: DMS oxidation and sulfur aerosol formation in the marine troposphere:
728 a focus on reactive halogen and multiphase chemistry, Atmos. Chem. Phys., 18(18), 13617–13637, doi:10.5194/acp-18-
729 13617-2018, 2018.
- 730 Chevrier, F.: Chauffage au bois et qualité de l'air en Vallée de l'Arve : définition d'un système de surveillance et impact
731 d'une politique de rénovation du parc des appareils anciens., PhD Thesis, Université Grenoble Alpes, Grenoble. [online]
732 Available from: <https://tel.archives-ouvertes.fr/tel-01527559> (Accessed 28 June 2018), 2016.
- 733 Colette, A., Menut, L., Haefelin, M. and Morille, Y.: Impact of the transport of aerosols from the free troposphere towards
734 the boundary layer on the air quality in the Paris area, Atmospheric Environment, 42(2), 390–402,
735 doi:10.1016/j.atmosenv.2007.09.044, 2008.
- 736 Daellenbach, K. R., Kourtchev, I., Vogel, A. L., Bruns, E. A., Jiang, J., Petäjä, T., Jaffrezo, J.-L., Aksoyoglu, S., Kalberer,
737 M., Baltensperger, U., El Haddad, I. and Prévôt, A. S. H.: Impact of anthropogenic and biogenic sources on the seasonal
738 variation in the molecular composition of urban organic aerosols: a field and laboratory study using ultra-high-resolution
739 mass spectrometry, Atmos. Chem. Phys., 19(9), 5973–5991, doi:10.5194/acp-19-5973-2019, 2019.
- 740 Dai, Q., Liu, B., Bi, X., Wu, J., Liang, D., Zhang, Y., Feng, Y. and Hopke, P. K.: Dispersion Normalized PMF Provides
741 Insights into the Significant Changes in Source Contributions to PM_{2.5} after the COVID-19 Outbreak, Environ. Sci.
742 Technol., acs.est.0c02776, doi:10.1021/acs.est.0c02776, 2020a.
- 743 Dai, Q., Hopke, P. K., Bi, X. and Feng, Y.: Improving apportionment of PM_{2.5} using multisite PMF by constraining G-
744 values with a priori information, Science of The Total Environment, 736, 139657, doi:10.1016/j.scitotenv.2020.139657,
745 2020b.

- 746 van Drooge, B. L. and Grimalt, J. O.: Particle size-resolved source apportionment of primary and secondary organic tracer
747 compounds at urban and rural locations in Spain, *Atmos. Chem. Phys.*, 15(13), 7735–7752, doi:10.5194/acp-15-7735-2015,
748 2015.
- 749 Emami, F. and Hopke, P. K.: Effect of adding variables on rotational ambiguity in positive matrix factorization solutions,
750 *Chemometrics and Intelligent Laboratory Systems*, 162, 198–202, doi:10.1016/j.chemolab.2017.01.012, 2017.
- 751 Favez, O., El Haddad, I., Piot, C., Boréave, A., Abidi, E., Marchand, N., Jaffrezo, J.-L., Besombes, J.-L., Personnaz, M.-B.,
752 Sciaire, J., Wortham, H., George, C. and D'Anna, B.: Inter-comparison of source apportionment models for the estimation of
753 wood burning aerosols during wintertime in an Alpine city (Grenoble, France), *Atmos. Chem. Phys.*, 10(12), 5295–5314,
754 doi:10.5194/acp-10-5295-2010, 2010.
- 755 Feng, J., Li, M., Zhang, P., Gong, S., Zhong, M., Wu, M., Zheng, M., Chen, C., Wang, H. and Lou, S.: Investigation of the
756 sources and seasonal variations of secondary organic aerosols in PM2.5 in Shanghai with organic tracers, *Atmospheric*
757 *Environment*, 79, 614–622, doi:10.1016/j.atmosenv.2013.07.022, 2013.
- 758 Franchini, M. and Mannucci, P.: Particulate Air Pollution and Cardiovascular Risk: Short-term and Long-term Effects,
759 *Semin Thromb Hemost*, 35(07), 665–670, doi:10.1055/s-0029-1242720, 2009.
- 760 Gelencsér, A., May, B., Simpson, D., Sánchez-Ochoa, A., Kasper-Giebl, A., Puxbaum, H., Caseiro, A., Pio, C. and Legrand,
761 M.: Source apportionment of PM2.5 organic aerosol over Europe: Primary/secondary, natural/anthropogenic, and
762 fossil/biogenic origin, *J. Geophys. Res.*, 112(D23), D23S04, doi:10.1029/2006JD008094, 2007.
- 763 Gianini, M. F. D., Fischer, A., Gehrig, R., Ulrich, A., Wichser, A., Piot, C., Besombes, J.-L. and Hueglin, C.: Comparative
764 source apportionment of PM10 in Switzerland for 2008/2009 and 1998/1999 by Positive Matrix Factorisation, *Atmospheric*
765 *Environment*, 54, 149–158, doi:10.1016/j.atmosenv.2012.02.036, 2012.
- 766 Golly, B., Waked, A., Weber, S., Samake, A., Jacob, V., Conil, S., Rangognio, J., Chrétien, E., Vagnot, M.-P., Robic, P.-Y.,
767 Besombes, J.-L. and Jaffrezo, J.-L.: Organic markers and OC source apportionment for seasonal variations of PM2.5 at 5
768 rural sites in France, *Atmospheric Environment*, 198, 142–157, doi:10.1016/j.atmosenv.2018.10.027, 2019.
- 769 Graham, B., Guyon, P., Taylor, P. E., Artaxo, P., Maenhaut, W., Glovsky, M. M., Flagan, R. C. and Andreae, M. O.:
770 Organic compounds present in the natural Amazonian aerosol: Characterization by gas chromatography-mass spectrometry:
771 ORGANIC COMPOUNDS IN AMAZONIAN AEROSOLS, *J. Geophys. Res.*, 108(D24), n/a-n/a,
772 doi:10.1029/2003JD003990, 2003.
- 773 Heo, J., Dulger, M., Olson, M. R., McGinnis, J. E., Shelton, B. R., Matsunaga, A., Sioutas, C. and Schauer, J. J.: Source
774 apportionments of PM2.5 organic carbon using molecular marker Positive Matrix Factorization and comparison of results
775 from different receptor models, *Atmospheric Environment*, 73, 51–61, doi:10.1016/j.atmosenv.2013.03.004, 2013.
- 776 Hopke, P. K.: Review of receptor modeling methods for source apportionment, *Journal of the Air & Waste Management
777 Association*, 66(3), 237–259, doi:10.1080/10962247.2016.1140693, 2016.
- 778 Horne, J. R. and Dabdub, D.: Impact of global climate change on ozone, particulate matter, and secondary organic aerosol
779 concentrations in California: A model perturbation analysis, *Atmospheric Environment*, 153, 1–17,
780 doi:10.1016/j.atmosenv.2016.12.049, 2017.
- 781 Hu, D., Bian, Q., Lau, A. K. H. and Yu, J. Z.: Source apportioning of primary and secondary organic carbon in summer PM
782 _{2.5} in Hong Kong using positive matrix factorization of secondary and primary organic tracer data, *J. Geophys. Res.*,
783 115(D16), D16204, doi:10.1029/2009JD012498, 2010.

- 784 Hyder, M., Genberg, J., Sandahl, M., Swietlicki, E. and Jönsson, J. Å.: Yearly trend of dicarboxylic acids in organic aerosols
785 from south of Sweden and source attribution, *Atmospheric Environment*, 57, 197–204, doi:10.1016/j.atmosenv.2012.04.027,
786 2012.
- 787 Ishizuka, T., Kabashima, H., Yamaguchi, T., Tanabe, K. and Hattori, H.: Initial Step of Flue Gas DesulfurizationAn IR
788 Study of the Reaction of SO₂ with NO_x on CaO⁻, *Environ. Sci. Technol.*, 34(13), 2799–2803, doi:10.1021/es991073p,
789 2000.
- 790 Jardine, K., Yañez-Serrano, A. M., Williams, J., Kunert, N., Jardine, A., Taylor, T., Abrell, L., Artaxo, P., Guenther, A.,
791 Hewitt, C. N., House, E., Florentino, A. P., Manzi, A., Higuchi, N., Kesselmeier, J., Behrendt, T., Veres, P. R., Derstroff, B.,
792 Fuentes, J. D., Martin, S. T. and Andreae, M. O.: Dimethyl sulfide in the Amazon rain forest: DMS in the Amazon, *Global
793 Biogeochem. Cycles*, 29(1), 19–32, doi:10.1002/2014GB004969, 2015.
- 794 Ke, L., Liu, W., Wang, Y., Russell, A. G., Edgerton, E. S. and Zheng, M.: Comparison of PM2.5 source apportionment using
795 positive matrix factorization and molecular marker-based chemical mass balance, *Science of The Total Environment*, 394(2–
796 3), 290–302, doi:10.1016/j.scitotenv.2008.01.030, 2008.
- 797 Kleindienst, T. E., Jaoui, M., Lewandowski, M., Offenberg, J. H., Lewis, C. W., Bhave, P. V. and Edney, E. O.: Estimates of
798 the contributions of biogenic and anthropogenic hydrocarbons to secondary organic aerosol at a southeastern US location,
799 *Atmospheric Environment*, 41(37), 8288–8300, doi:10.1016/j.atmosenv.2007.06.045, 2007.
- 800 Kunit, M. and Puxbaum, H.: Enzymatic determination of the cellulose content of atmospheric aerosols, *Atmospheric
801 Environment*, 30(8), 1233–1236, doi:10.1016/1352-2310(95)00429-7, 1996.
- 802 Langrish, J. P., Bosson, J., Unoosson, J., Muala, A., Newby, D. E., Mills, N. L., Blomberg, A. and Sandström, T.:
803 Cardiovascular effects of particulate air pollution exposure: time course and underlying mechanisms, *Journal of Internal
804 Medicine*, 272(3), 224–239, doi:10.1111/j.1365-2796.2012.02566.x, 2012.
- 805 Lee, S., Liu, W., Wang, Y., Russell, A. G. and Edgerton, E. S.: Source apportionment of PM2.5: Comparing PMF and CMB
806 results for four ambient monitoring sites in the southeastern United States, *Atmospheric Environment*, 42(18), 4126–4137,
807 doi:10.1016/j.atmosenv.2008.01.025, 2008.
- 808 Li, S.-M., Barrie, L. A., Talbot, R. W., Harriss, R. C., Davidson, C. I. and Jaffrezo, J.-L.: Seasonal and geographic variations
809 of methanesulfonic acid in the arctic troposphere, *Atmospheric Environment. Part A. General Topics*, 27(17–18), 3011–
810 3024, doi:10.1016/0960-1686(93)90333-T, 1993.
- 811 Marmur, A., Mulholland, J. A. and Russell, A. G.: Optimized variable source-profile approach for source apportionment,
812 *Atmospheric Environment*, 41(3), 493–505, doi:10.1016/j.atmosenv.2006.08.028, 2007.
- 813 McNeill, V. F.: Atmospheric Aerosols: Clouds, Chemistry, and Climate, *Annu. Rev. Chem. Biomol. Eng.*, 8(1), 427–444,
814 doi:10.1146/annurev-chembioeng-060816-101538, 2017.
- 815 Miyazaki, Y., Fu, P. Q., Kawamura, K., Mizoguchi, Y. and Yamanoi, K.: Seasonal variations of stable carbon isotopic
816 composition and biogenic tracer compounds of water-soluble organic aerosols in a deciduous forest, *Atmos. Chem. Phys.*,
817 12(3), 1367–1376, doi:10.5194/acp-12-1367-2012, 2012.
- 818 Norris, G., Duvall, R., Brown, S. and Bai, S.: Positive Matrix Factorization (PMF) 5.0 Fundamentals and User Guide, , 136,
819 2014.

- 820 Ostro, B., Tobias, A., Querol, X., Alastuey, A., Amato, F., Pey, J., Pérez, N. and Sunyer, J.: The Effects of Particulate Matter
821 Sources on Daily Mortality: A Case-Crossover Study of Barcelona, Spain, Environmental Health Perspectives, 119(12),
822 1781–1787, doi:10.1289/ehp.1103618, 2011.
- 823 Paatero, P.: The Multilinear Engine—A Table-Driven, Least Squares Program for Solving Multilinear Problems, Including
824 the n -Way Parallel Factor Analysis Model, Journal of Computational and Graphical Statistics, 8(4), 854–888,
825 doi:10.1080/10618600.1999.10474853, 1999.
- 826 Paatero, P. and Tapper, U.: Positive matrix factorization: A non-negative factor model with optimal utilization of error
827 estimates of data values, Environmetrics, 5(2), 111–126, doi:10.1002/env.3170050203, 1994.
- 828 Pachon, J. E., Balachandran, S., Hu, Y., Weber, R. J., Mulholland, J. A. and Russell, A. G.: Comparison of SOC estimates
829 and uncertainties from aerosol chemical composition and gas phase data in Atlanta, Atmospheric Environment, 44(32),
830 3907–3914, doi:10.1016/j.atmosenv.2010.07.017, 2010.
- 831 Pandolfi, M., Mooibroek, D., Hopke, P., van Pinxteren, D., Querol, X., Herrmann, H., Alastuey, A., Favez, O., Hüglin, C.,
832 Perdrix, E., Riffault, V., Sauvage, S., van der Swaluw, E., Tarasova, O. and Colette, A.: Long-range and local air pollution:
833 what can we learn from chemical speciation of particulate matter at paired sites?, Atmos. Chem. Phys., 20(1), 409–429,
834 doi:10.5194/acp-20-409-2020, 2020.
- 835 Pernigotti, D. and Belis, C. A.: DeltaSA tool for source apportionment benchmarking, description and sensitivity analysis,
836 Atmospheric Environment, 180, 138–148, doi:10.1016/j.atmosenv.2018.02.046, 2018.
- 837 Pernigotti, D., Belis, C. A. and Spanò, L.: SPECIEUROPE: The European data base for PM source profiles, Atmospheric
838 Pollution Research, 7(2), 307–314, doi:10.1016/j.apr.2015.10.007, 2016.
- 839 Petit, J.-E., Pallarès, C., Favez, O., Alleman, L. Y., Bonnaire, N. and Rivière, E.: Sources and Geographical Origins of PM10
840 in Metz (France) Using Oxalate as a Marker of Secondary Organic Aerosols by Positive Matrix Factorization Analysis,
841 Atmosphere, 10(7), 370, doi:10.3390/atmos10070370, 2019.
- 842 Pey, J., Alastuey, A. and Querol, X.: PM10 and PM2.5 sources at an insular location in the western Mediterranean by using
843 source apportionment techniques, Science of The Total Environment, 456–457, 267–277,
844 doi:10.1016/j.scitotenv.2013.03.084, 2013.
- 845 Pindado, O. and Perez, R. M.: Source apportionment of particulate organic compounds in a rural area of Spain by positive
846 matrix factorization, Atmospheric Pollution Research, 2(4), 492–505, doi:10.5094/APR.2011.056, 2011.
- 847 Putaud, J.-P., Van Dingenen, R., Alastuey, A., Bauer, H., Birmili, W., Cyrys, J., Flentje, H., Fuzzi, S., Gehrig, R., Hansson,
848 H. C., Harrison, R. M., Herrmann, H., Hitzenberger, R., Hüglin, C., Jones, A. M., Kasper-Giebl, A., Kiss, G., Kousa, A.,
849 Kuhlbusch, T. A. J., Löschnau, G., Maenhaut, W., Molnar, A., Moreno, T., Pekkanen, J., Perrino, C., Pitz, M., Puxbaum, H.,
850 Querol, X., Rodriguez, S., Salma, I., Schwarz, J., Smolik, J., Schneider, J., Spindler, G., ten Brink, H., Tursic, J., Viana, M.,
851 Wiedensohler, A. and Raes, F.: A European aerosol phenomenology – 3: Physical and chemical characteristics of particulate
852 matter from 60 rural, urban, and kerbside sites across Europe, Atmospheric Environment, 44(10), 1308–1320,
853 doi:10.1016/j.atmosenv.2009.12.011, 2010.
- 854 Puxbaum, H.: Size distribution and seasonal variation of atmospheric cellulose, Atmospheric Environment, 37(26), 3693–
855 3699, doi:10.1016/S1352-2310(03)00451-5, 2003.
- 856 Qiao, F., Li, Q. and Lei, Y.: Particulate Matter Caused Health Risk in an Urban Area of the Middle East and the Challenges
857 in Reducing its Anthropogenic Emissions, Environ Pollut Climate Change, 02(01), doi:10.4172/2573-458X.1000145, 2018.

- 858 Saeaw, N. and Thepanondh, S.: Source apportionment analysis of airborne VOCs using positive matrix factorization in
859 industrial and urban areas in Thailand, *Atmospheric Pollution Research*, 6(4), 644–650, doi:10.5094/APR.2015.073, 2015.
- 860 Samake, A., Jaffrezo, J.-L., Favez, O., Weber, S., Jacob, V., Albinet, A., Riffault, V., Perdrix, E., Waked, A., Golly, B.,
861 Salameh, D., Chevrier, F., Oliveira, D. M., Besombes, J.-L., Martins, J. M. F., Conil, S., Guillaud, G., Meshba, B., Rocq, B.,
862 Robic, P.-Y., Hulin, A., Meur, S. L., Descheemaeker, M., Chretien, E. and Uzu, G.: Polyols and glucose particulate species
863 as tracers of primary biogenic organic aerosols at 28 french sites, *Atmospheric Chemistry and Physics Discussions*, 1–23,
864 doi:<https://doi.org/10.5194/acp-2018-773>, 2018.
- 865 Samaké, A., Jaffrezo, J.-L., Favez, O., Weber, S., Jacob, V., Albinet, A., Riffault, V., Perdrix, E., Waked, A., Golly, B.,
866 Salameh, D., Chevrier, F., Oliveira, D. M., Bonnaire, N., Besombes, J.-L., Martins, J. M. F., Conil, S., Guillaud, G., Mesbah,
867 B., Rocq, B., Robic, P.-Y., Hulin, A., Le Meur, S., Descheemaeker, M., Chretien, E., Marchand, N. and Uzu, G.: Polyols
868 and glucose particulate species as tracers of primary biogenic organic aerosols at 28 French sites, *Atmos. Chem. Phys.*,
869 19(5), 3357–3374, doi:10.5194/acp-19-3357-2019, 2019.
- 870 Schauer, J. J. and Cass, G. R.: Source Apportionment of Wintertime Gas-Phase and Particle-Phase Air Pollutants Using
871 Organic Compounds as Tracers, *Environ. Sci. Technol.*, 34(9), 1821–1832, doi:10.1021/es981312t, 2000.
- 872 Schneider, W. F., Li, J. and Hass, K. C.: Combined Computational and Experimental Investigation of SO_x Adsorption on
873 MgO , *J. Phys. Chem. B*, 105(29), 6972–6979, doi:10.1021/jp010747r, 2001.
- 874 Seinfeld, J. H. and Pankow, J. F.: ORGANIC ATMOSPHERIC PARTICULATE MATERIAL, *Annu. Rev. Phys. Chem.*,
875 54(1), 121–140, doi:10.1146/annurev.physchem.54.011002.103756, 2003.
- 876 Shiraiwa, M., Ueda, K., Pozzer, A., Lammel, G., Kampf, C. J., Fushimi, A., Enami, S., Arangio, A. M., Fröhlich-Nowoisky,
877 J., Fujitani, Y., Furuyama, A., Lakey, P. S. J., Lelieveld, J., Lucas, K., Morino, Y., Pöschl, U., Takahama, S., Takami, A.,
878 Tong, H., Weber, B., Yoshino, A. and Sato, K.: Aerosol Health Effects from Molecular to Global Scales, *Environ. Sci.
879 Technol.*, 51(23), 13545–13567, doi:10.1021/acs.est.7b04417, 2017.
- 880 Srivastava, M. K., Subramanian, R., Rogge, W. F. and Robinson, A. L.: Sources of organic aerosol: Positive matrix
881 factorization of molecular marker data and comparison of results from different source apportionment models, *Atmospheric
882 Environment*, 41(40), 9353–9369, doi:10.1016/j.atmosenv.2007.09.016, 2007.
- 883 Srivastava, D., Favez, O., Perraudin, E., Villenave, E. and Albinet, A.: Comparison of Measurement-Based Methodologies to
884 Apportion Secondary Organic Carbon (SOC) in PM_{2.5}: A Review of Recent Studies, *Atmosphere*, 9(11), 452,
885 doi:10.3390/atmos9110452, 2018a.
- 886 Srivastava, D., Tomaz, S., Favez, O., Lanzafame, G. M., Golly, B., Besombes, J.-L., Alleman, L. Y., Jaffrezo, J.-L., Jacob,
887 V., Perraudin, E., Villenave, E. and Albinet, A.: Speciation of organic fraction does matter for source apportionment. Part 1:
888 A one-year campaign in Grenoble (France), *Science of The Total Environment*, 624, 1598–1611,
889 doi:10.1016/j.scitotenv.2017.12.135, 2018b.
- 890 Szmigielski, R., Surratt, J. D., Gómez-González, Y., Van der Veken, P., Kourtchev, I., Vermeylen, R., Blockhuys, F., Jaoui,
891 M., Kleindienst, T. E., Lewandowski, M., Offenberg, J. H., Edney, E. O., Seinfeld, J. H., Maenhaut, W. and Claeys, M.: 3-
892 methyl-1,2,3-butanetricarboxylic acid: An atmospheric tracer for terpene secondary organic aerosol, *Geophys. Res. Lett.*,
893 34(24), L24811, doi:10.1029/2007GL031338, 2007.
- 894 Ullerstam, M., Vogt, R., Langer, S. and Ljungström, E.: The kinetics and mechanism of SO_2 oxidation by O_3 on mineral
895 dust, *Phys. Chem. Chem. Phys.*, 4(19), 4694–4699, doi:10.1039/B203529B, 2002.

- 896 Ullerstam, M., Johnson, M. S., Vogt, R. and Ljungström, E.: DRIFTS and Knudsen cell study of the heterogeneous reactivity
897 of SO₂ and NO₂ on mineral dust, *Atmos. Chem. Phys.*, 3(6), 2043–2051, doi:10.5194/acp-3-2043-2003, 2003.
- 898 Usher, C. R., Al-Hosney, H., Carlos-Cuellar, S. and Grassian, V. H.: A laboratory study of the heterogeneous uptake and
899 oxidation of sulfur dioxide on mineral dust particles: UPTAKE OF SULFUR DIOXIDE ON DUST, *J.-Geophys.-Res.*,
900 107(D23), ACH 16-1-ACH 16-9, doi:10.1029/2002JD002051, 2002.
- 901 Verma, S. K., Kawamura, K., Chen, J. and Fu, P.: Thirteen years of observations on primary sugars and sugar alcohols over
902 remote Chichijima Island in the western North Pacific, *Atmos. Chem. Phys.*, 18(1), 81–101, doi:10.5194/acp-18-81-2018,
903 2018.
- 904 Vlachou, A., Tobler, A., Lamkaddam, H., Canonaco, F., Daellenbach, K. R., Jaffrezo, J.-L., Minguillón, M. C., Maasikmets,
905 M., Teinemaa, E., Baltensperger, U., El Haddad, I. and Prévôt, A. S. H.: Development of a versatile source apportionment
906 analysis based on positive matrix factorization: a case study of the seasonal variation of organic aerosol sources in Estonia,
907 *Atmos. Chem. Phys. Discuss.*, 1–21, doi:10.5194/acp-2018-1099, 2018.
- 908 Waked, A., Favez, O., Alleman, L. Y., Piot, C., Petit, J.-E., Delaunay, T., Verlinden, E., Golly, B., Besombes, J.-L., Jaffrezo,
909 J.-L. and Leoz-Garziandia, E.: Source apportionment of PM₁₀ in a north-western Europe regional
910 urban background site (Lens, France) using positive matrix factorization and including primary biogenic emissions, *Atmos.*
911 *Chem. Phys.*, 14(7), 3325–3346, doi:10.5194/acp-14-3325-2014, 2014.
- 912 Wang, Q., He, X., Huang, X. H. H., Griffith, S. M., Feng, Y., Zhang, T., Zhang, Q., Wu, D. and Yu, J. Z.: Impact of
913 Secondary Organic Aerosol Tracers on Tracer-Based Source Apportionment of Organic Carbon and PM_{2.5}: A Case Study in
914 the Pearl River Delta, China, *ACS Earth Space Chem.*, 1(9), 562–571, doi:10.1021/acsearthspacechem.7b00088, 2017a.
- 915 Wang, Q., He, X., Huang, X. H. H., Griffith, S. M., Feng, Y., Zhang, T., Zhang, Q., Wu, D. and Yu, J. Z.: Impact of
916 Secondary Organic Aerosol Tracers on Tracer-Based Source Apportionment of Organic Carbon and PM_{2.5}: A Case Study in
917 the Pearl River Delta, China, *ACS Earth Space Chem.*, 1(9), 562–571, doi:10.1021/acsearthspacechem.7b00088, 2017b.
- 918 Wang, Y., Hopke, P. K., Xia, X., Rattigan, O. V., Chalupa, D. C. and Utell, M. J.: Source apportionment of airborne
919 particulate matter using inorganic and organic species as tracers, *Atmospheric Environment*, 55, 525–532,
920 doi:10.1016/j.atmosenv.2012.03.073, 2012.
- 921 Warneck, P.: Chemistry of the natural atmosphere, 2nd ed., Academic Press, San Diego., 2000.
- 922 Weber, S., Uzu, G., Calas, A., Chevrier, F., Besombes, J.-L., Charron, A., Salameh, D., Ježek, I., Močnik, G. and Jaffrezo,
923 J.-L.: An apportionment method for the oxidative potential of atmospheric particulate matter sources: application to a one-
924 year study in Chamonix, France, *Atmos. Chem. Phys.*, 18(13), 9617–9629, doi:10.5194/acp-18-9617-2018, 2018.
- 925 Weber, S., Salameh, D., Albinet, A., Alleman, L. Y., Waked, A., Besombes, J.-L., Jacob, V., Guillaud, G., Meshbah, B.,
926 Rocq, B., Hulin, A., Dominik-Sègue, M., Chrétien, E., Jaffrezo, J.-L. and Favez, O.: Comparison of PM10 Sources Profiles
927 at 15 French Sites Using a Harmonized Constrained Positive Matrix Factorization Approach, *Atmosphere*, 10(6), 310,
928 doi:10.3390/atmos10060310, 2019.
- 929 Willers, S. M., Eriksson, C., Gidhagen, L., Nilsson, M. E., Pershagen, G. and Bellander, T.: Fine and coarse particulate air
930 pollution in relation to respiratory health in Sweden, *Eur Respir J*, 42(4), 924–934, doi:10.1183/09031936.00088212, 2013.
- 931 Wilson, R. and Spengler, J. D., Eds.: Particles in our air: concentrations and health effects, Harvard School of Public Health ;
932 distributed by Harvard University Press, Cambridge, Mass., 1996.

- 933 Yang, F., Kawamura, K., Chen, J., Ho, K., Lee, S., Gao, Y., Cui, L., Wang, T. and Fu, P.: Anthropogenic and biogenic
934 organic compounds in summertime fine aerosols (PM_{2.5}) in Beijing, China, *Atmospheric Environment*, 124, 166–175,
935 doi:10.1016/j.atmosenv.2015.08.095, 2016.
- 936 Yuan, Z., Lau, A., Zhang, H., Yu, J., Louie, P. and Fung, J.: Identification and spatiotemporal variations of dominant PM₁₀
937 sources over Hong Kong, *Atmospheric Environment*, 40(10), 1803–1815, doi:10.1016/j.atmosenv.2005.11.030, 2006.
- 938 Zhang, Y., Müller, L., Winterhalter, R., Moortgat, G. K., Hoffmann, T. and Pöschl, U.: Seasonal cycle and temperature
939 dependence of pinene oxidation products, dicarboxylic acids and nitrophenols in fine and coarse air particulate matter,
940 *Atmos. Chem. Phys. Discuss.*, 10(5), 13253–13286, doi:10.5194/acpd-10-13253-2010, 2010.
- 941 Zheng, J., Tan, M., Shibata, Y., Tanaka, A., Li, Y., Zhang, G., Zhang, Y. and Shan, Z.: Characteristics of lead isotope ratios
942 and elemental concentrations in PM₁₀ fraction of airborne particulate matter in Shanghai after the phase-out of leaded
943 gasoline, *Atmospheric Environment*, 38(8), 1191–1200, doi:10.1016/j.atmosenv.2003.11.004, 2004.
- 944 Zhu, Y., Huang, L., Li, J., Ying, Q., Zhang, H., Liu, X., Liao, H., Li, N., Liu, Z., Mao, Y., Fang, H. and Hu, J.: Sources of
945 particulate matter in China: Insights from source apportionment studies published in 1987–2017, *Environment International*,
946 115, 343–357, doi:10.1016/j.envint.2018.03.037, 2018.

947